CR - 118917

INFLUENCE OF GASEOUS HYDROGEN ON METALS

INTERIM REPORT

by

R. J. Walter

H. G. Hayes

W. T. Chandler

ROCKETDYNE

A DIVISION OF NORTH AMERICAN ROCKWELL CORPORATION

prepared for

George C. Marshall Space Flight Center
Marshall Space Flight Center, Alabama 35812

R-8719

INFLUENCE OF GASEOUS HYDROGEN ON METALS

INTERIM REPORT

24 May 1971

by

R. J. Walter

H. G. Hayes

W. T. Chandler

Prepared Under Contract NAS8-25579

for

George C. Marshall Space Flight Center
Marshall Space Flight Center, Alabama 35812

by

Advanced Programs
Rocketdyne
A Division of North American Rockwell Corporation
Canoga Park, California

FOREWORD

This report was prepared by the Advanced Programs Division of Rocketdyne, a Division of North American Rockwell Corporation, in compliance with National Aeronautics and Space Administration Contract NAS8-25579, and covers the period from 5 May 1970 through 4 May 1971. The work was sponsored by the George C. Marshall Space Flight Center, Alabama, with Mr. W. B. McPherson acting as project monitor and Mr. T. A. Coultas as the Rocketdyne Program Manager.

Mr. D. A. Pearson performed fracture toughness tests and Messrs. G. E. Dyer and J. Testa assisted with tensile and fracture toughress tests. Mr. Testa also performed the metallographic work. Dr. R. P. Jewett provided helpful technical discussions.

ABSTRACT

Embrittlement of Inconel 718 by 5,000 psi hydrogen at room temperature was found to vary considerably with condition. Reduction of notch tensile properties was least for material with a very fine grain size, moderate for a coarse grained material after a 1925, 1400-1200 F heat treatment, and most severe for a coarse grained material after a 1725, 1325-1150 F heat treatment. Embrittlement appeared to correlate with grain size and the presence of a nearly continuous precipitate tentatively identified as Ni_3Cb. The weld metal and heat-affected-zone of Inconel 718 welds was more embrittled by hydrogen than was the parent metal. Fracture toughness tests gave K_{th} values for coarse grained Inconel 718 in 5,000 psi hydrogen at room temperatures of approximately 21 KSI $\sqrt{in}$ for the 1725, 1325-1150 F heat treatment and 50 KSI $\sqrt{in}$ for the 1925, 1400-1200 F heat treatment.

The tensile properties of Inconel 625 were considerably reduced by 5,000 psi at room temperature, but there was no effect at -200 F. The tensile properties of AISI 321 stainless were slightly reduced by 5,000 psi hydrogen both at room temperature and -200 F. The tensile properties of Ti-5Al-2.5Sn ELI were essentially unaffected by hydrogen at -200 F. The room temperature fracture toughness of AISI 321 stainless steel, Inconel 625, and Ti-5Al-2.5Sn ELI were reduced by 5,000 psi hydrogen, but considerable plastic blunting of the crack occurred in AISI 321 stainless steel and crack branching occurred in Inconel 625. The fracture toughness tests conducted on A-286 stainless steel and 2219-T87 aluminum alloy and the tensile and fracture toughness tests conducted on OFHC copper showed no embrittlement from exposure to 5,000 psi hydrogen.

CONTENTS

FIGURES

TABLES

APPENDIX

INTRODUCTION

The space shuttle vehicle will be propelled by high performance, high chamber pressure rocket engines using oxygen and hydrogen propellants, and the hydrogen pressures in the space shuttle main engine (SSME) will be higher than encountered in previous production engines.

It has been shown (Ref. 1-11) that high-pressure hydrogen seriously degrades the mechanical properties of many of the commonly used engineering alloys. Thus, data on the mechanical properties of candidate structural alloys in hydrogen under simulated space shuttle operating conditions are required to assist in the selection of alloys and, ultimately, to provide design data and safe operating parameters.

Inconel 718 has many attractive properties and is being considered for extensive use in the space shuttle main engine. In previous work (Ref. 1 and 4), it was found to be extremely embrittled by high-pressure hydrogen. However, the degree of embrittlement was found (Ref. 10) to vary significantly with the heat treatment and/or heat of Inconel 718 tested. Also, few data (Ref. 9) were available on the hydrogen-environment embrittlement of Inconel 718 weldments.

Other candidate materials for regions exposed to high-pressure hydrogen in the space shuttle include Inconel 625, AISI 321 stainless steel, Ti-5Al-2.5Sn ELI and OFHC copper. Previous work (Ref. 1 and 4) showed that Ti-5Al-2.5Sn ELI is severely embrittled and AISI 321 stainless steel is slightly embrittled by 10,000 psi hydrogen at ambient temperature. Inconel 625, being a nickel base alloy, would be expected to be embrittled from exposure to high pressure hydrogen environments. Walter and Chandler (Ref. 1 and 4) found that OFHC copper was not embrittled by exposure to 10,000 psi hydrogen, but investigations by Vennett and Ansell (Ref. 11) indicated some reduction of ductility of unnotched specimens of OFHC copper in ambient temperature, 10,000 psi hydrogen.

This program was performed to determine the gaseous hydrogen environment embrittlement of the metals indicated above under conditions of hydrogen pressure and temperature pertinent to the space shuttle. The program was divided into the following phases:

I. Variation of Hydrogen-Environment Embrittlement with Material Condition for Inconel 718.

Tensile tests on notched specimens were used to determine the effect of as-received material condition, heat treatment, and welding on the hydrogen-environment embrittlement of Inconel 718 in 5,000 psi hydrogen at room temperature.

II. Tensile Properties of Alloys in Hydrogen Environments.

The effect of 5,000 psi hydrogen on the tensile properties of the alloys listed above was determined at room temperature and -200 F.

III. Threshold Stress Intensity of Alloys in Hydrogen Environments.

Threshold stress intensities for the alloys listed above and in addition 2219-T87 aluminum alloy were determined with modified WOL specimens for a hydrogen pressure of 5,000 psi and room temperature.

EXPERIMENTAL PROCEDURES

MATERIALS

The chemical compositions, heat treatments, and mechanical properties of the test materials in the as-received conditions are listed in Tables 1, 2, and 3, respectively. The Inconel 718 rolled bar was supplied by the Allvac Division of Teledyne, the forging was fabricated by Carlton Forge Works, Inc. from a Special Metals Corporation ingot; and the plate was supplied by the Stellite Division of Cabot Corporation. Each heat of Inconel 718 was tested in 3 heat treatment conditions. These Inconel 718 heat treatments are listed in Table 4 and the corresponding room temperature mechanical properties in air are listed in Table 5.

Inconel 718 weldments were made using the 1/2-inch thick plate with a joint design shown in Fig. 1. The weldments were made by gas tungsten arc welding with Inconel 718 filler metal and with the weld perpendicular to the plate rolling direction. After each weld pass, the weld was die penetrant inspected and after the weldments were completed, the welded plates were x-rayed. No defects were found during these inspections.

TEST PROCEDURES AND APPARATUS

The tensile specimens for Phases I and II were fabricated with the longitudinal specimen axis parallel to the longitudinal rolling direction. The test specimens were 0.306 inch in diameter, 9 inches long, and were threaded for 1 inch on each end and had a 16-rms surface finish. For the unnotched specimens, a 1.25-inch long, 0.250-inch diameter gage section was used. The notched specimens had a 60^{0} V notch at the midpoint with a specimen diameter at the root of the notch of 0.150 + 0.001 inch. A

TABLE 1

CHEMICAL COMPOSITION (WEIGHT PERCENT) OF TEST MATERIALS
(SUPPLIER CERTIFICATION)

Material	C	S	Mn	Si	Cr	Mo	Ti	Al	Fe	Cu	Ni	P	Cb + Ta	Miscellaneous
Inconel 718														
1-1/4 in. x 2-3/4 in. Rolled Bar	.073	.004	.096	.17	18.82	2.98	.98	.49	Bal.	.03	51.68	.008	5.02	0.46 Co, 0.005 B
1-1/2 in. Forging	.05	.003	.10	.10	17.8	3.00	1.00	.57	18.5	.10	Bal.	.01	5.39	0.10 Co, 0.003 B
1/2 in. Plate	.06	.009	.12	.10	17.92	3.10	1.01	.52	Bal.	.01	52.77	.002	5.10	0.39 Co, 0.004 B
Inconel 625														
1-1/4 in. x 2-3/4 in. Rolled Bar	.047	.003	.05	.20	21.14	8.97	.11	.20	2.55		Bal.	.008	3.73 / .04	0.07 Co
A-286														
1-1/4 in. Forging	.048	.010	1.20	.63	14.15	1.25	2.21	.16	Bal.		24.88	.016		0.047 B, 0.01 Zr, 0.22 V
AISI 321 S.S.														
1-1/4 in. Plate	.060	.015	1.46	.58	17.80	.24	.51		Bal.	.12	10.45	.026		
Ti-5Al-2.5Sn ELI														
1-1/4 in. Plate	.022		.001				Bal.	5.1	.19					0.012 N_2, 0.010 H_2 0.08 O_2, 2.4 Sn
2219-T87 Al Alloy														
1-1/4 in. Plate			0.20-0.40	.20 max.				Bal.	0.30 max.	5.8-6.8				0.10-0.25 Zr, 0.05-0.15 V, 0.10 max.Zr, 0.02 max. Mg
OFHC Copper*														
1-1/4 in. Plate	Cu - 99.99 min. S - 0.0018 max. P - 0.003 max. Zn, Mn, As, Sb, Bi, Te, Sn, Se, Pb, O_2 - 0.001 max. each Hg, Cd - 0.0001 max. each													

*From Rocketdyne Spec. RB0170-047 - No Supplier Certification

TABLE 2

HEAT TREATMENT OF MATERIALS AS RECEIVED

MATERIAL	HEAT TREATMENT
Inconel 718	
a) 1-1/4 in. x 2-3/4 in Rolled Bar	1750 F, 1 Hour, Air Cooled
b) 1-1/2 in. Forging	1750 F, 1 Hour, Air Cooled
c) 1/2 in. Plate	1750 F, 30 Min., Spray Quenched
Inconel 625 1-1/4 in. x 2-3/4 in. Rolled Bar	1700 F, 1 Hour, Air Cooled
A-286 1-1/4 in. Forging	Solution Treated 1800 F, 1 Hour, Oil Cooled Aged 1325 F, 16 Hours, Air Cooled
AISI 321 SS 1-1/4 in. Plate	Hot Rolled, Annealed and Descaled
Ti-5Al-2.5Sn ELI 1-1/4 in. Plate	Final Anneal Cycle 1300-1400 F, 2-8 Hours, Air Cooled
2219-T87 Al Alloy 1-1/4 in. Plate	Solution 995 F, Cold Water Quench, Approx. 8% Cold Work, Age 24 Hours at 325 F
OFHC Copper 1-1/4 in. Plate	Annealed

TABLE 3

MECHANICAL PROPERTIES OF TEST MATERIALS AS RECEIVED
(SUPPLIER CERTIFICATION)

Material	Temp. °F	Yield Strength KSI	Tensile Strength KSI	Percent Reduction of Area	Percent Elongation	1200 F Stress Rupture Properties in AMS 5596 C Aged Condition
Inconel 718*						
1-1/4 in. x 2-3/4 in. Rolled Bar	RT	166	200	44	20	64.9 Hrs @ 110 KSI
	1200	140	165	43	16	5.6% El, 10% RA
1-1/2 in. Forging	RT	171	199	36	18	59.8 Hrs @ 112 KSI
	1200	146	158	36	12	5.5% El
1/2 in. Plate	RT	165	208		21	42 Hrs @ 110 KSI
	1200	147	170		17	12% El
Inconel 625						
1-1/4 in. x 2-3/4 in. Rolled Bar	RT	91	143	54	39	18 Hrs @ 18 KSI & 1500 F 69% El, 51% RA
A-286						
1-1/4 in. Forging	RT	113	150	33	23	
AISI 321 S.S.						
1-1/4 in. Plate	RT	49	89	66	46	
Ti-5Al-2.5Sn ELI						
1-1/4 in. Plate	RT	L 112	L 122	L 28.5	L 17	
	RT	T 119	T 124	T 39.5	T 16.5	
2219-T87 Al Alloy						
1-1/4 in. Plate	RT	57	70	18	10	
OFHC Copper						
1-1/4 in. Plate	None Supplied					

*Aged AMS 5596 C, 1325 F 8 Hrs, FC to 1150 F AC, Total Aging Time 18 Hrs.

TABLE 4

INCONEL 718 HEAT TREATMENTS

Heat Treatment	Solution Treatments		Aging Treatments					Total Aging Time, Hours
			First Aging		Time of Furnace Cooling to 2nd Aging Temp., Hrs.	Second Aging		
	Temperature F	Time Min.	Temperature F	Time Hrs.		Temperature F	Time Hrs.	
A	1725	60	1325	8	3-4	1150	6-7½	18-18½
B	1725	60	1500	10	1-4	1200	6-8½	20-21
C	1925	20*	1400	10	2-4½	1200	6-8	20-20½

*The Inconel 718 welded specimens were solution annealed 60 minutes at 1925 F instead of the usual 20 minutes.

TABLE 5

TENSILE PROPERTIES OF HEAT TREATED UNNOTCHED INCONEL 718
SPECIMENS TESTED IN AIR AT 1 ATM PRESSURE

	Heat Treatment			Tensile Properties			
		Aging Temp.		Strength		Ductility	
Material	Solution Temperature F	First F	Second F	Yield KSI	Ultimate KSI	Percent Reduction of Area	Percent Elongation in 1-1/4 in. Red. Sec.
1-1/4 in. x	1725	1325	1150	163	202	35	23
2-3/4 in.	1725	1500	1200	127	182	32	24
Rolled Bar	1925	1400	1200	161	195	37	26
1-1/2 in.	1725	1325	1150	159	198	31	22
Forging	1725	1500	1200	124	178	35	25
	1925	1400	1200	169	198	41	26
1/2 in. Plate	1725	1325	1150	159	205	36	23
	1725	1500	1200	133	189	35	23
	1925	1400	1200	167	204	38	25
Weldment in 1/2	1725	1325	1150	150	173	12	4.4*
in. Thick	1725	1500	1200	126	166	13	7.3*
Plate	1925	1400	1200	165	199	23	13*

*Reduced Section 0.65 in. Long.

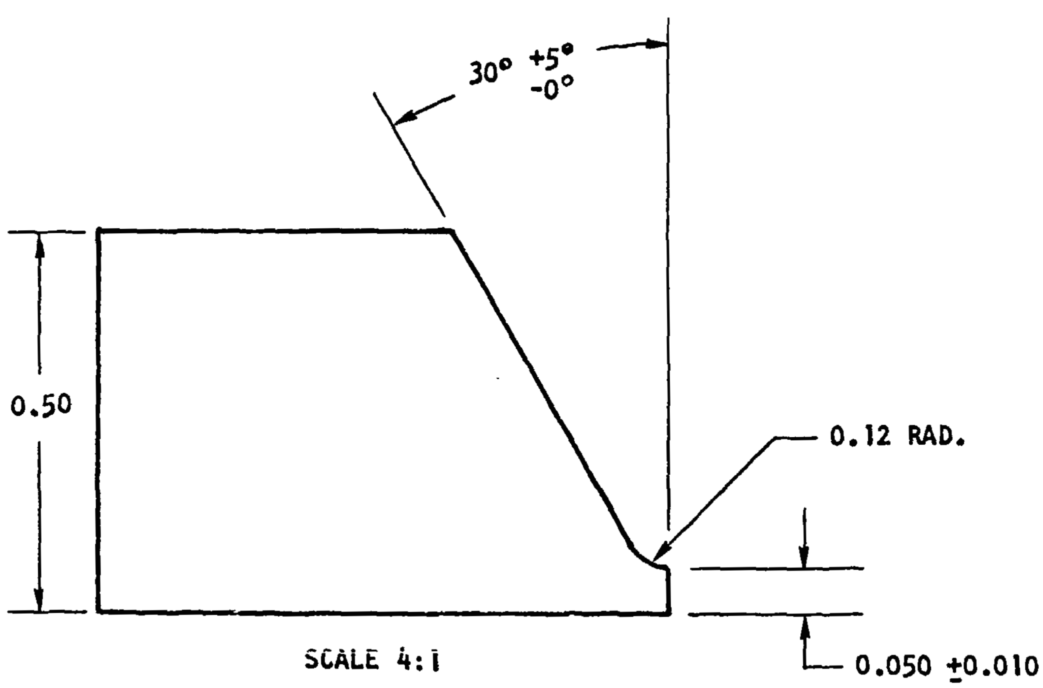

Figure 1. Weld Design for Gas Tungsten Arc Welding of Inconel 718 With Inconel 718 Filler Metal

root radius of 0.00095 was used to obtain an elastic stress concentration factor (K_t) of approximately 8.4. The stress concentration factor was calculated according to Peterson (Ref. 12).

Notched welded specimens were fabricated with the longitudinal specimen axis parallel to the rolling direction and with the notches located in either the weld or in the heat affected zone. In addition, the unnotched tensile properties of the Inconel 718 weldments were determined in air. The reduced sections of these specimens were 0.65 inches long bridging the approximately 1/4-inch long weldment.

The apparatus used for performing the tensile tests has been described elsewhere (Ref. 4). Briefly, the tensile specimens were enclosed in a small pressure vessel with the ends of the specimens extending outside the vessel through sliding seals. The load was applied to the specimen by a hydraulic ram. The unnotched specimens were cross head paced at 0.005 in./min. Notched specimens were load paced at a loading rate that corresponds to 0.0007/min strain rate.

Tests with this apparatus were conducted at room temperature and -200 F. For the cryogenic tests, the pressure vessel was surrounded by a dewar filled with cold nitrogen. The nitrogen was cooled by passing through copper coils immersed in liquid nitrogen and was fed into the dewar at a rate sufficient to maintain the specimen temperature at -200 F.

Calculation of the actual tensile load for test specimens required that the friction from the sliding seals and the tensile load from the high-pressure gas be considered. The following equation was used to calculate the ultimate load of the unnotched specimens:

Ultimate Load = Applied Load - Friction + Pressure
x (Specimen Area at Sliding Seal -
Specimen Area Prior to Necking)

The maximum combined tensile load was assumed to occur prior to necking. For notched specimens, the original area at the base of the notch was used in place of the "area prior to necking" in the above equation.

The percent elongation of the unnotched specimens was measured between punch marks placed 2 inches apart outside and bridging the reduced section. The reduction of area of notched specimens was determined by using an optical comparator to measure the cross section of the notch before and after testing.

The method selected for determining threshold stress intensity (K_{TH}) in high-pressure hydrogen was patterned after one developed by Novak and Rolfe (Ref. 13) who used a modified WOL specimen. The specimen designs used in this program are shown in Figs. 2 and 3. The specimens were oriented in the TL material direction, i.e., the loading direction was parallel to the long transverse direction in the material and the cracks propagated parallel to the longitudinal rolling direction.

The Novak and Rolfe technique involves maintaining a constant crack opening displacement (COD) and allowing the load, and thus the stress intensity, to decrease as the crack extends. The crack grows until the stress intensity equals K_{TH} in the environment and the crack growth stops. At the end of the test, the load at crack arrest is determined by measuring the COD, unloading

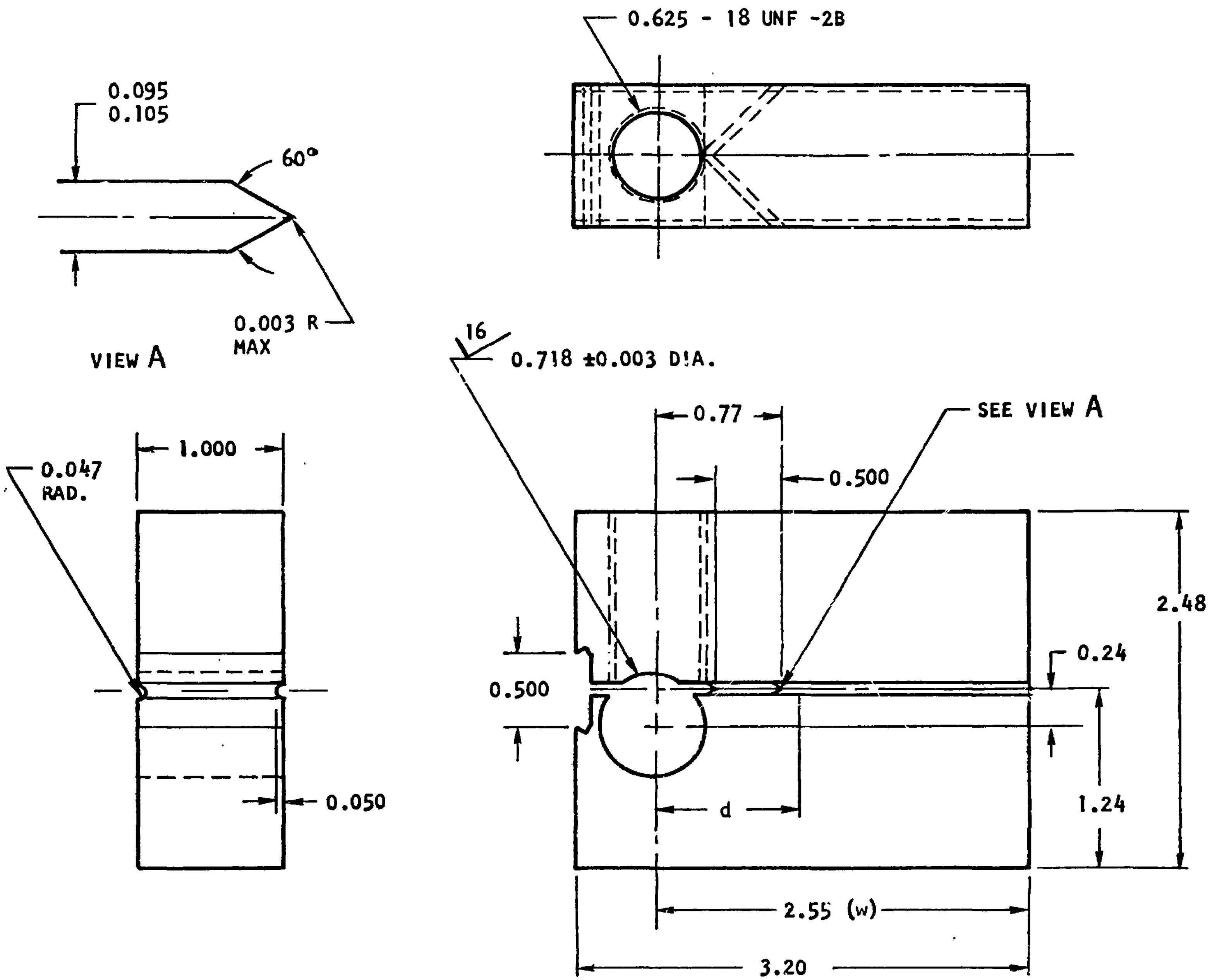

Figure 2. Modified WOL Specimen With Chevron Notch

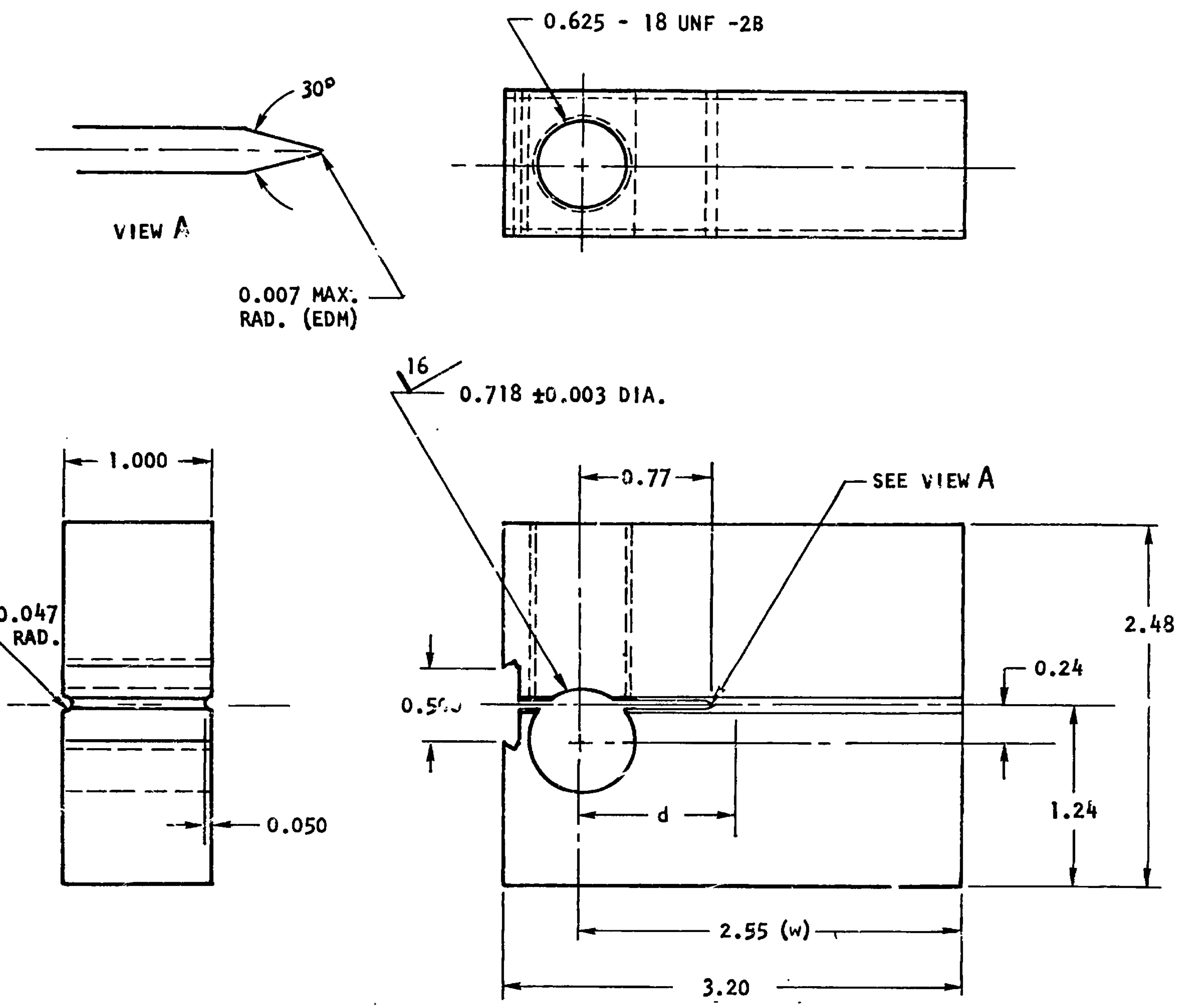

Figure 3. Modified WOL Specimen With Straight EDM Notch

the specimen, and then reloading the specimen to the measured COD on a tensile machine. The specimen is then usually fatigue marked, fractured, and the crack length measured. From the crack length and a previously experimentally determined relationship between compliance, i.e., the relationship between COD and applied load, and crack length, the crack arrest load can be calculated and compared with the measured load. Novak and Rolfe (Ref. 13) derived the following equation for calculating the stress intensity for the specimen shown in Fig. 2 and 3.

$$K = \frac{PC_3\left(\frac{a}{w}\right)}{\sqrt{B\,B_n}\,(a)^{1/2}}$$

where

P = applied load, kips

$$C_3\left(\frac{a}{w}\right) = 30.96\left(\frac{a}{w}\right) - 195.8\left(\frac{a}{w}\right)^2 + 730.6\left(\frac{a}{w}\right)^3 - 1186.3\left(\frac{a}{w}\right)^4 + 754.6\left(\frac{a}{w}\right)^5$$

a = effective crack length, in.

w = specimen dimension, in. (2.55 in.)

B = specimen thickness, in. (1 in.)

B_n = net specimen thickness, in. (0.90 in.)

The effective crack length was determined from the following relationship:

$$a = \frac{a_1 + a_5 + 2\,(a_2 + a_3 + a_4)}{8}$$

where a_1 and a_5 are the crack lengths measured at points 0.015 inch in from the face notches along the 2 sides.

a_3 is the crack length at the center thickness

a_2 is the crack length midway between a_1 and a_3

a_4 is the crack length midway between a_3 and a_5

In order to assure that crack growth occurs in the crack plane, the modified WOL specimen was side notched as shown in Fig. 2. A chevron notch (Fig. 2) and a straight notch produced by electrical discharge machining (Fig. 3) were used to obtain a straight crack front in the WOL specimens.

The Novak-Rolfe technique was modified for performing the threshold stress intensity measurements in the high pressure hydrogen environment. It was considered important that the load exerted on the specimen be monitored continually during the test. From the load dropoff, the displacement at which crack growth initiates and the time at which the threshold has been reached can be ascertained. Thus, it is possible to preload a specimen just to that level needed for crack growth, which is desirable for preventing excessive crack branching. Secondly, the load at threshold can be determined directly without subsequent reloading, which is usually required for obtaining the crack opening displacement at threshold. This is particularly important for tests conducted at other than room temperature, because the COD at the test temperature and the load to obtain this COD at that temperature must otherwise be measured.

In order to achieve continual load monitoring, a special apparatus*, shown in Fig. 4, was used which involved measuring the load by means of two load cells. By rotating the loading ram, a compressive force was exerted across the load cells, and this force in turn acts as a tension load across the specimen.

This apparatus was placed inside a pressure vessel, shown in the schematic in Fig. 5 and the photograph in Fig. 6. The vessel is constructed of A-286, a precipitation hardened austenitic stainless steel, and is capable of 6,000 psi hydrogen pressure at cryogenic and elevated temperatures (-320 F to 1200 F).

Figure 7 schematically shows the loading apparatus inside the pressure vessel. The loading ram which is rotated to load the specimen extends out of the vessel through sliding seals located in the water-cooled neck. The specimens were held from turning by the two bolts at the bottom of the apparatus. When the vessel is pressurized, the pressure acts to push the loading ram through the sliding seals out of the vessel. In order that this pressure load was not transmitted to the specimen, the loading ram was held in place by means of a sleeve located between the torque shaft coupler and the inside vessel top. The two bolts at the bottom of the vessel were loosened so that the sleeve takes the entire pressure load.

The displacement was monitored during the test by means of NASA-type clip-on gage positioned on the specimen in the usual manner.

---

* The use of dual load cells in this manner for measuring the load was suggested by Transducers, Inc., Santa Fe Springs, California 90670.

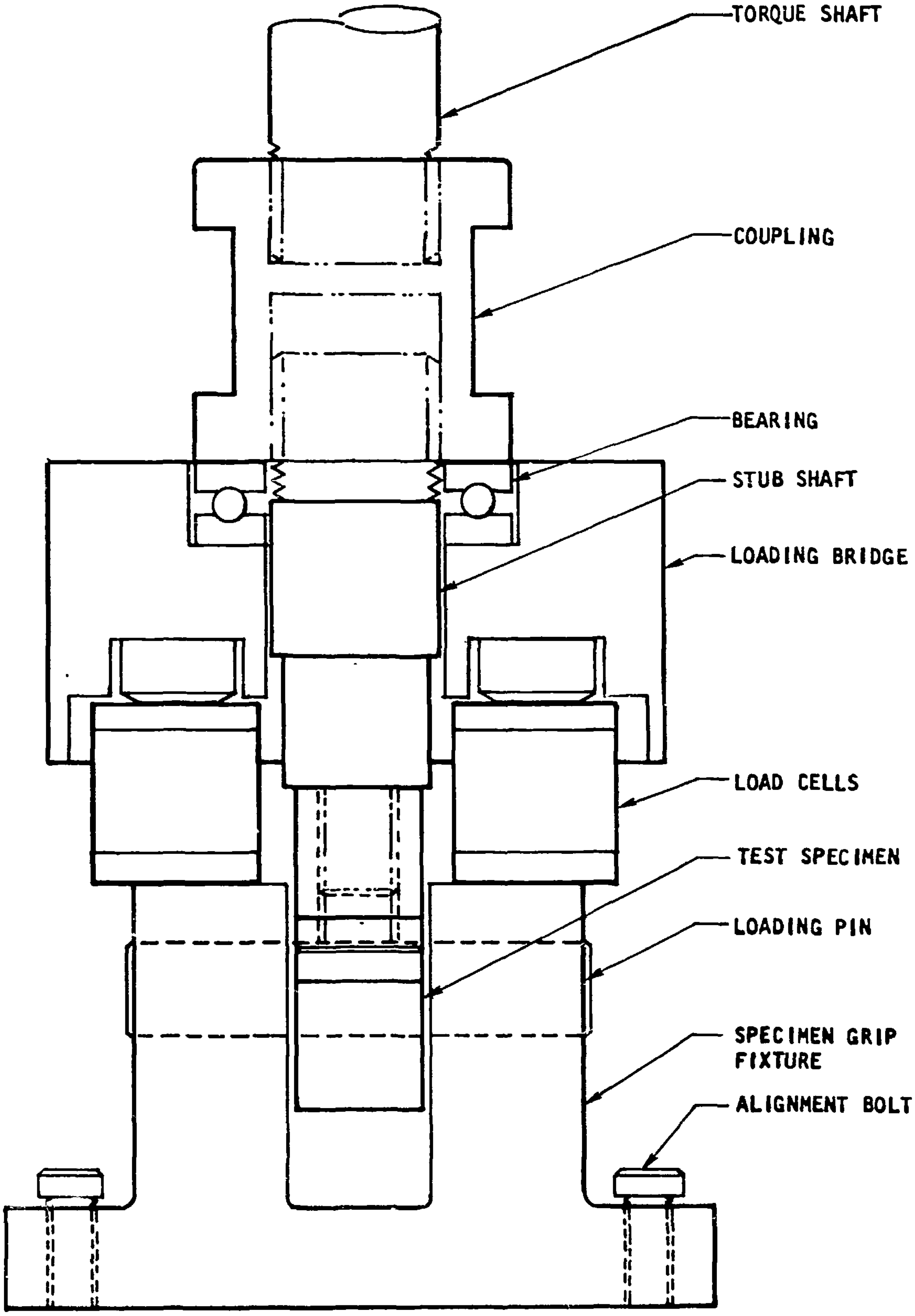

Figure 4. Apparatus for Holding a Constant Deflection and Measuring the Load on the WOL Specimen

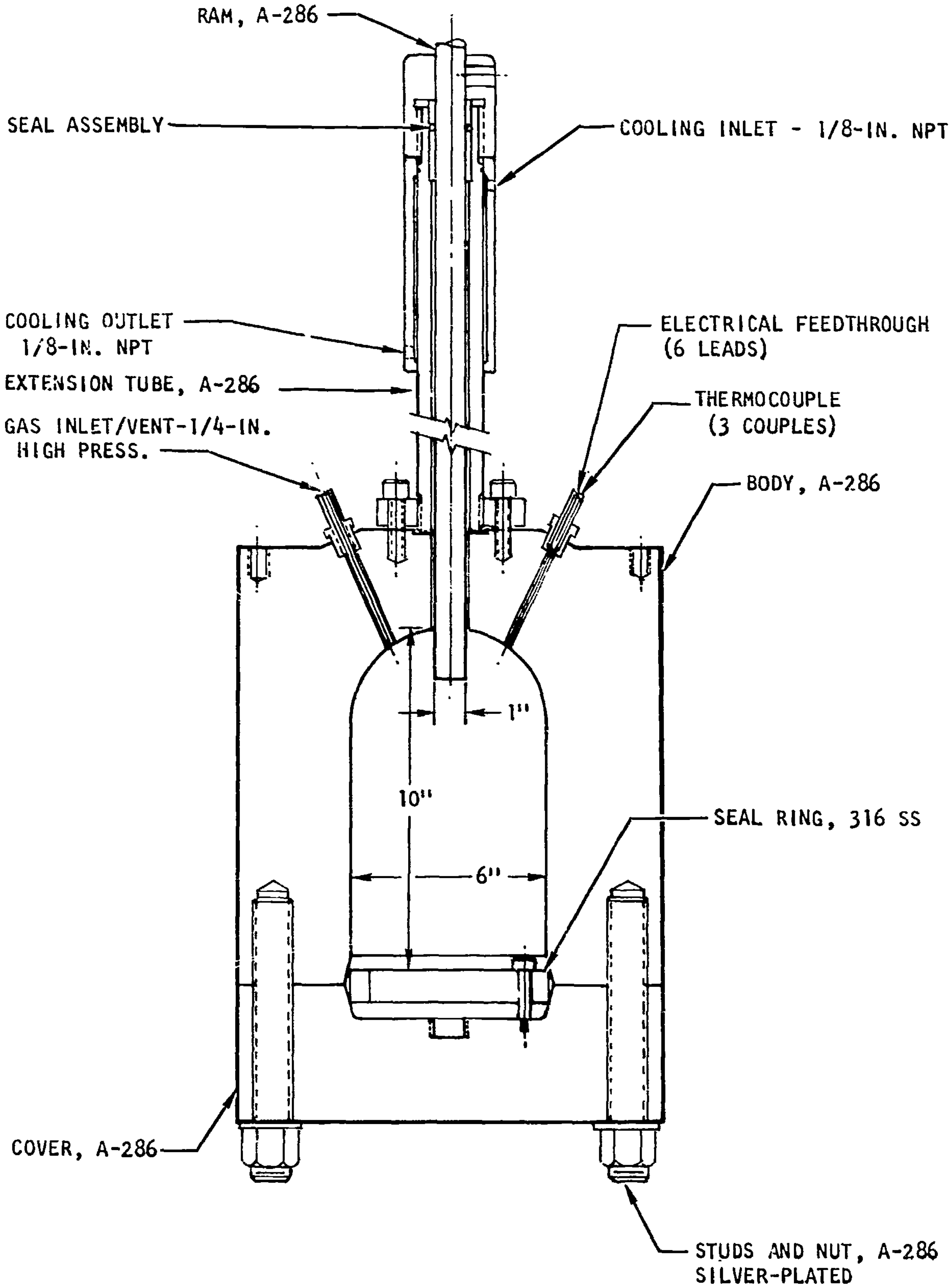

Figure 5. Pressure Vessel Used to Perform Tests on Modified WOL Specimen in High-Pressure Hydrogen

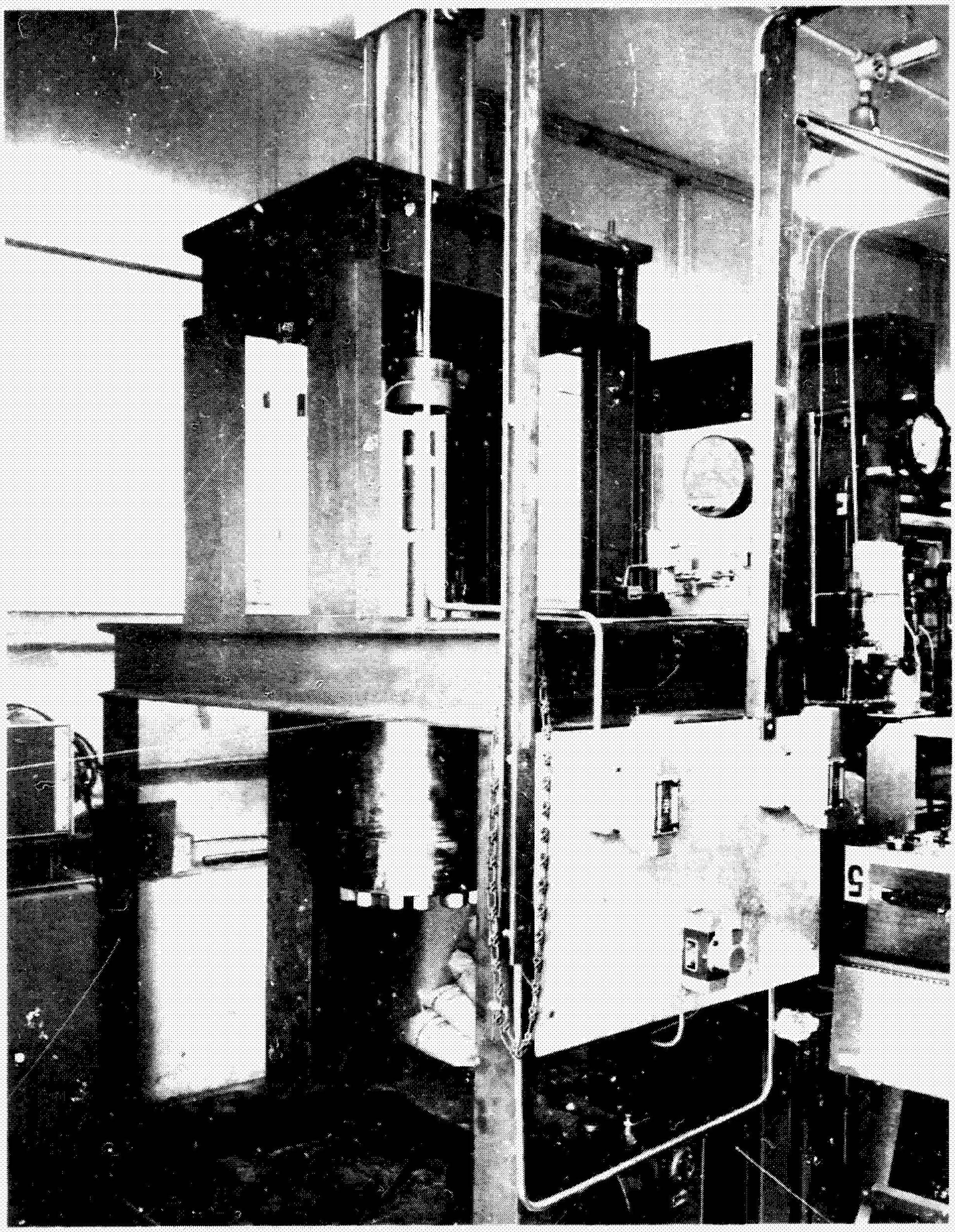

1ST92-11/23/70-C1E

Figure 6. Test Frame and Pressure Vessel for Performing Tests on Modified WOL Specimens in High-Pressure Hydrogen

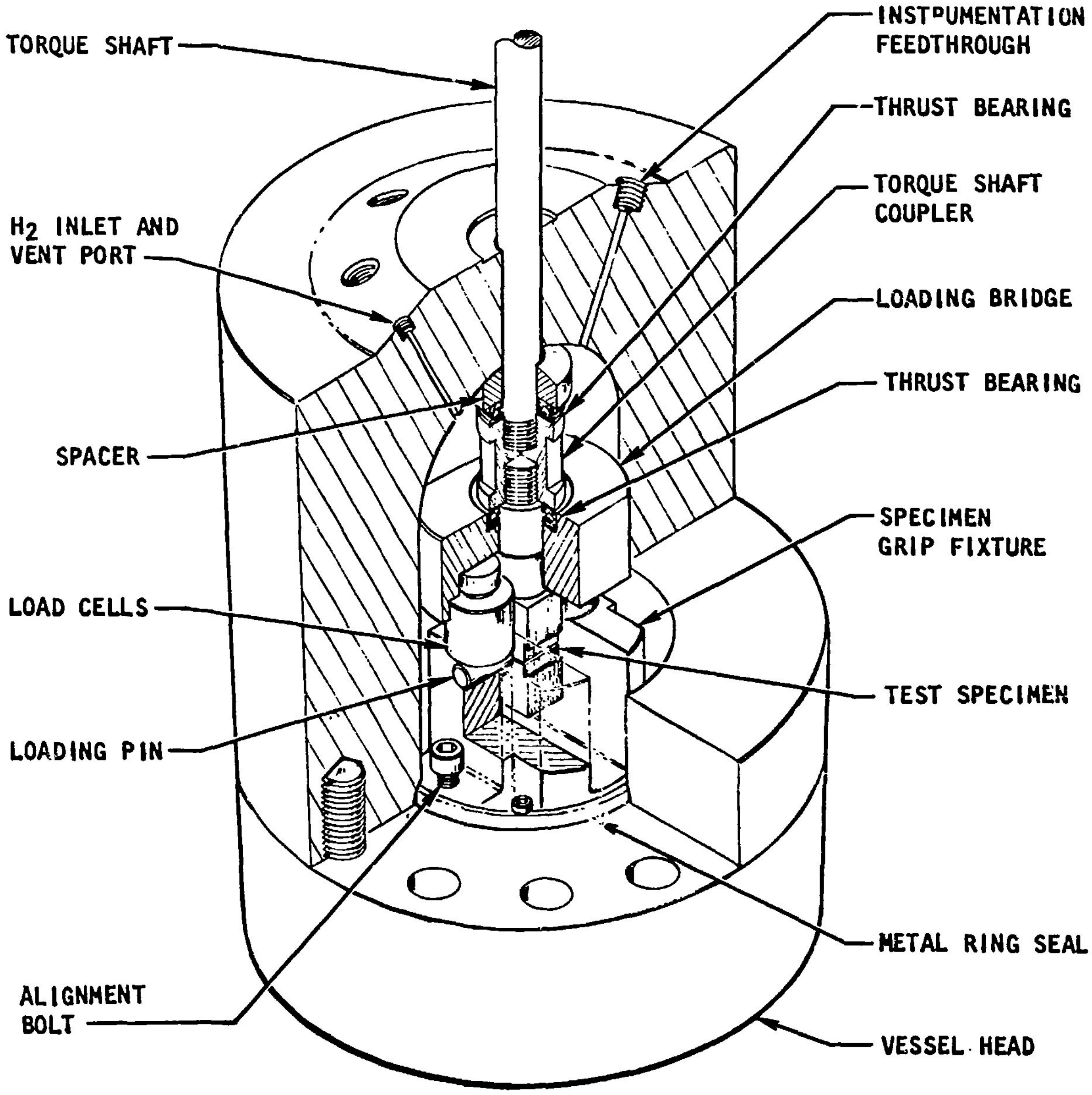

Figure 7. Apparatus for Performing Threshold Stress Intensity Measurements

It was important that the loading apparatus be designed so that none of the components add impurities to the high purity hydrogen environment. Threaded connections were vented to allow evacuation of these regions. To lower friction at the coupling, $MoSi_2$ dry lubricant, which has a very low vapor pressure and is inert to hydrogen, was baked onto the threads. Teflon was used as the electrical wire insulators.

Considerable care was used so that the hydrogen test environment for the tensile and fracture toughness measurements was not contaminated. High-purity bottled hydrogen was further purified by passing through an Engelhard DeOxo unit, BaO desiccant, and a mixture of activated charcoal and activated alumina maintained at boiling nitrogen temperature. To remove air from the pressure vessels used for performing the tensile tests, the vessels were evacuated to $<$ 20 microns and backfilled 3 times to 100 psi hydrogen followed each time by $<$ 20 microns evacuation. This was then followed by 5 pressurizations to 5,000 psi hydrogen-depressurization to about 50 psi hydrogen before the final pressurization to the 5,000 psi hydrogen test pressure. The pressure vessel used for performing the threshold measurements was evacuated to $<$ 20 microns and backfilled 3 times to 1,000 psi followed each time by evacuation to $<$ 20 microns. This was then followed by three 2,000 psi to 200 psi hydrogen pressurization-depressurizations before final pressurization to the 5,000 psi hydrogen test pressure.

Purity of the hydrogen after pressurization with a diaphragm compressor was analyzed to be 0.6 ppm N_2, 0.1-0.2 ppm O_2 with no measureable H_2O and CO_2. Bottled helium with typical impurity contents of 3 ppm O_2, 1 ppm H_2O, and 6 to 7 ppm N_2 was used for the comparison tests.

RESULTS AND DISCUSSION

VARIATION OF HYDROGEN-ENVIRONMENT EMBRITTLEMENT WITH MATERIAL CONDITION FOR INCONEL 718

Tensile Tests of Notched Inconel 718 Specimens

Table 6 contains the average results of the tensile tests on notched specimens of Inconel 718 in various conditions in 5,000 psi hydrogen and 5,000 psi helium at room temperature. The data for individual specimens are presented in Appendix A. It is apparent from these results that hydrogen-environment embrittlement of Inconel 718 is considerably affected by the material condition.

Consider first the results for the specimens without welds. The least hydrogen environment embrittlement, i.e., the highest N_{H_2}/N_{He} ratio (0.86), occurred with the 1725, 1325-1150 F and 1725, 1500-1200 F heat treatments of the plate. On the other hand, the greatest embrittled (N_{H_2}/N_{He} = 0.54-0.59) resulted from the 1725, 1325-1150 F heat treatment of the rolled bar and forging and the 1725, 1500-1200 F heat treatment of the forging. Intermediate embrittlement (N_{H_2}/N_{He} = 0.70-0.77) resulted from the 1925, 1400-1200 F heat treatment of all three starting materials and from the 1725, 1500-1200 F heat treatment of the rolled bar. Of the three heat treatments, the 1925, 1400-1200 F heat treatment gave the most consistent results with N_{H_2}/N_{He} being 0.71, 0.76, and 0.77 for the rolled bar, forging, and plate, respectively. Of the three forms of material, i.e., rolled bar, forging, and plate, the plate had the lowest and most consistent hydrogen-environment embrittlement for the three heat treatment conditions.

Although the least embrittlement occurred with the plate with the 1725, 1325-1150 F heat treatment, the notched strength in hydrogen was the same

TABLE 6

EFFECT OF 5,000 PSI H_2 AT ROOM TEMPERATURE ON THE AVERAGE PROPERTIES OF NOTCHED SPECIMENS OF INCONEL 718 IN VARIOUS CONDITIONS

Heat Treatment*					Notch Properties**		
Solution Temp. °F	Aging Temp. °F First	Aging Temp. °F Second	Material	Environment (5,000 psi)	Strength KSI	N_{H_2}/N_{He}	Reduction of Area %
1725	1325	1150	1-1/4 in. x 2-3/4 in. Rolled Bar	Helium	283	--	2.9
				Hydrogen	152	0.54	0.9
			1-1/2 in. Forging	Helium	290	--	3.0
				Hydrogen	170	0.59	1.1
			1/2 in. Plate	Helium	287	--	3.0
				Hydrogen	246	0.86	2.0
			1/2 in. Plate - Weld Metal	Helium	206	--	1.4
				Hydrogen	163	0.79	1.0
			1/2 in. Plate - Weld HAZ	Helium	265	--	1.8
				Hydrogen	168	0.63	0.7
1725	1500	1200	1-1/4 in. x 2-3/4 in. Rolled Bar	Helium	240	--	2.9
				Hydrogen	168	0.70	1.8
			1-1/2 in. Forging	Helium	253	--	2.2
				Hydrogen	144	0.57	1.2
			1/2 in. Plate	Helium	251	--	2.7
				Hydrogen	217	0.86	2.1

TABLE 6

(CONTINUED)

Heat Treatment*			Material	Environment (5,000 psi)	Notch Properties**		
Solution Temp. °F	Aging Temp. °F First	Aging Temp. °F Second			Strength KSI	N_{H_2}/N_{He}	Reduction of Area %
1725	1500	1200	1/2 in. Plate - Weld Metal	Helium	180	--	2.1
				Hydrogen	140	0.78	0.6
			1/2 in. Plate - Weld HAZ	Helium	202	--	1.4
				Hydrogen	152	0.75	1.1
1925	1400	1200	1-1/4 in. x 2-3/4 in. Rolled Bar	Helium	322	--	5.0
				Hydrogen	230	0.71	1.7
			1-1/2 in. Forging	Helium	339	--	4.6
				Hydrogen	258	0.76	1.8
			1/2 in. Plate	Helium	320	--	3.7
				Hydrogen	247	0.77	2.3
			1/2 in. Plate - Weld Metal	Helium	268	--	2.6
				Hydrogen	151	0.56	0.8
			1/2 in. Plate - Weld HAZ	Helium	301	--	3.8
				Hydrogen	217	0.72	1.1

*Complete heat treatments given in Table 4.

**K_t = 8.7

for the plate with the 1925, 1400-1200 F heat treatment as for the plate with the 1725, 1325-1150 F heat treatment. The lower N_{H_2}/N_{He} ratio with the 1925, 1400-1200 F heat treatment resulted from the higher notched strength in helium. In fact, for all three forms, rolled bar, forging, and plate, the 1925, 1400-1200 F heat treatment resulted in the highest notch strength both in helium and in hydrogen.

The investigation of the hydrogen-environment embrittlement of welds was made only with the 1/2 in. plate which, as it turned out, was the least embrittled of the forms tested. The welds were tested only in the heat treated after welding condition. For all three heat treatments, the notch strength in both helium and hydrogen was lower for the weld metal and the heat-affected-zone than for the parent metal.

Also, in all cases, the degree of hydrogen environment embrittlement was greater for the weld metal and heat-affected-zone than for the parent metal. The weld metal and the heat-affected-zone with the 1725, 1500-1200 F heat treatment were embrittled by hydrogen to about the same degree. For the 1725, 1325-1150 F heat treatment, the heat-affected-zone was more embrittled by hydrogen than was the weld metal while the reverse was true for the 1925, 1400-1200 F heat treatment. The most severe hydrogen-environment embrittlement in weld specimens was for weld metal with the 1925, 1400-1200 F heat treatment. As with the parent metal, the notch strength in helium of both the weld metal and heat-affected-zone was higher with the 1925, 1400-1200 F heat treatment than with the other two heat treatments. However, the degree of hydrogen-environment embrittlement of the weld metal was large enough for the 1925, 1400-1200 F heat treatment that the notch strength in hydrogen was somewhat lower with that heat treatment than with the 1725, 1325-1150 F heat treatment.

Metallography of Inconel 718

Optical and electron microscopy was performed on specimens of the Inconel 718 bar, forging, and plates in the three heat treatment conditions. Photomicrographs of Inconel 718 in the 1750 F annealed, as-received condition are shown for the rolled bar in Fig. 8 and for the forging and plate in Fig. 9. Since the microstructures of longitudinal and transverse sections of the plate and forging were the same for this and subsequent heat treatments, only the transverse section photomicrographs are shown for these materials. There were considerable differences among the as-received grain structure resulting from the three processing methods. The structure of the rolled bar was duplex with the larger grains elongated in the rolling direction. The grain sizes of the forging and plate were relatively uniform. The grain size of the forging was relatively large (ASTM 4-1/2). The plate was fine grained (ASTM 8-1/2).

Photomicrographs of bar, forging, and plate specimens with the 1725 F, 1325-1150 F heat treatment are shown in Fig. 10 and with the 1725, 1500-1200 F heat treatment in Fig. 11 and 12. The microstructures resulting from these heat treatments appear virtually the same as those for the 1750 F annealed, as received condition.

Figure 13 shows photomicrographs of Inconel 718 bar, forging, and plate in the 19[illegible]5 F, 1400-1200 F heat treatment condition. Recrystallization and grain growth occurred during the heat treatment, and the microstructural appearance, including grain size, were the same for all three forms.

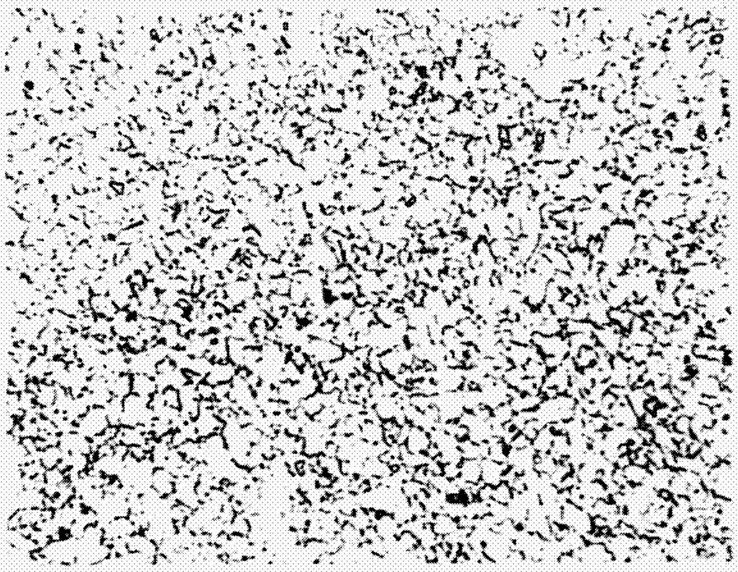

200x

Transverse Cross Section

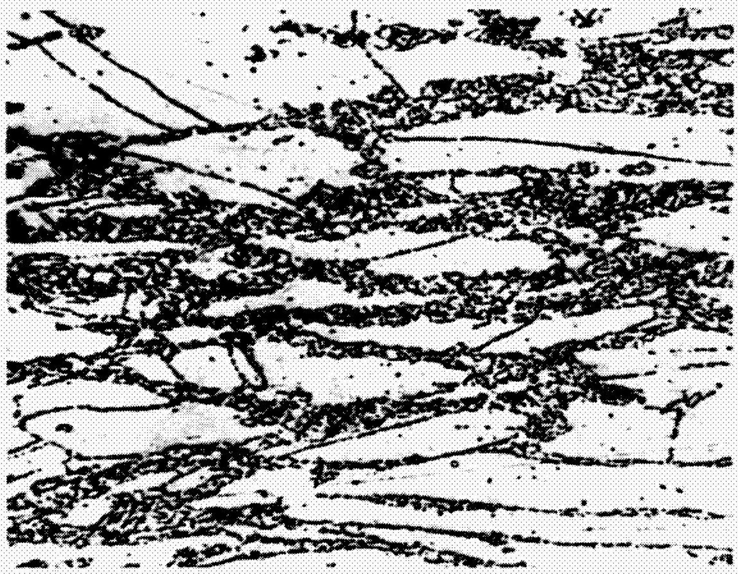

200x

Longitudinal Cross Section

Figure 8. Photomicrographs of Inconel 718 Rolled Bar in the 1750 F Solution Annealed, as Received Condition. Etchant: 92 HCl, 3 HNO_3, 1/2 H_2SO_4

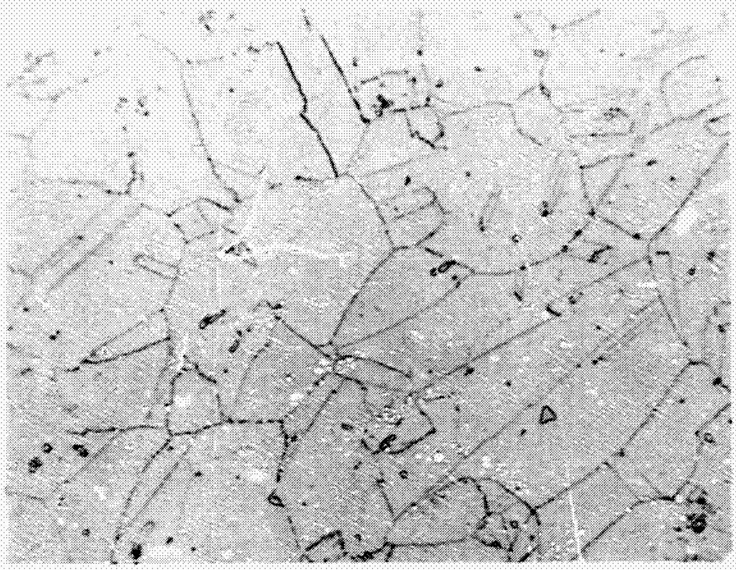

200x

Forging

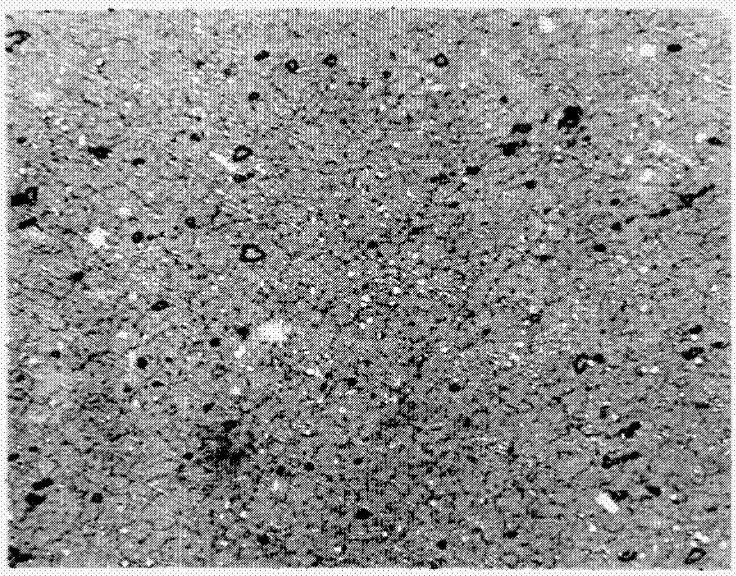

200x

Plate

Figure 9. Photomicrographs of Transverse Sections of Inconel 718 Forging and Plate in 1750 F Solution Annealed, as Received Condition. Etchant: 92 HCl, 3 HNO_3, 1/2 H_2SO_4.

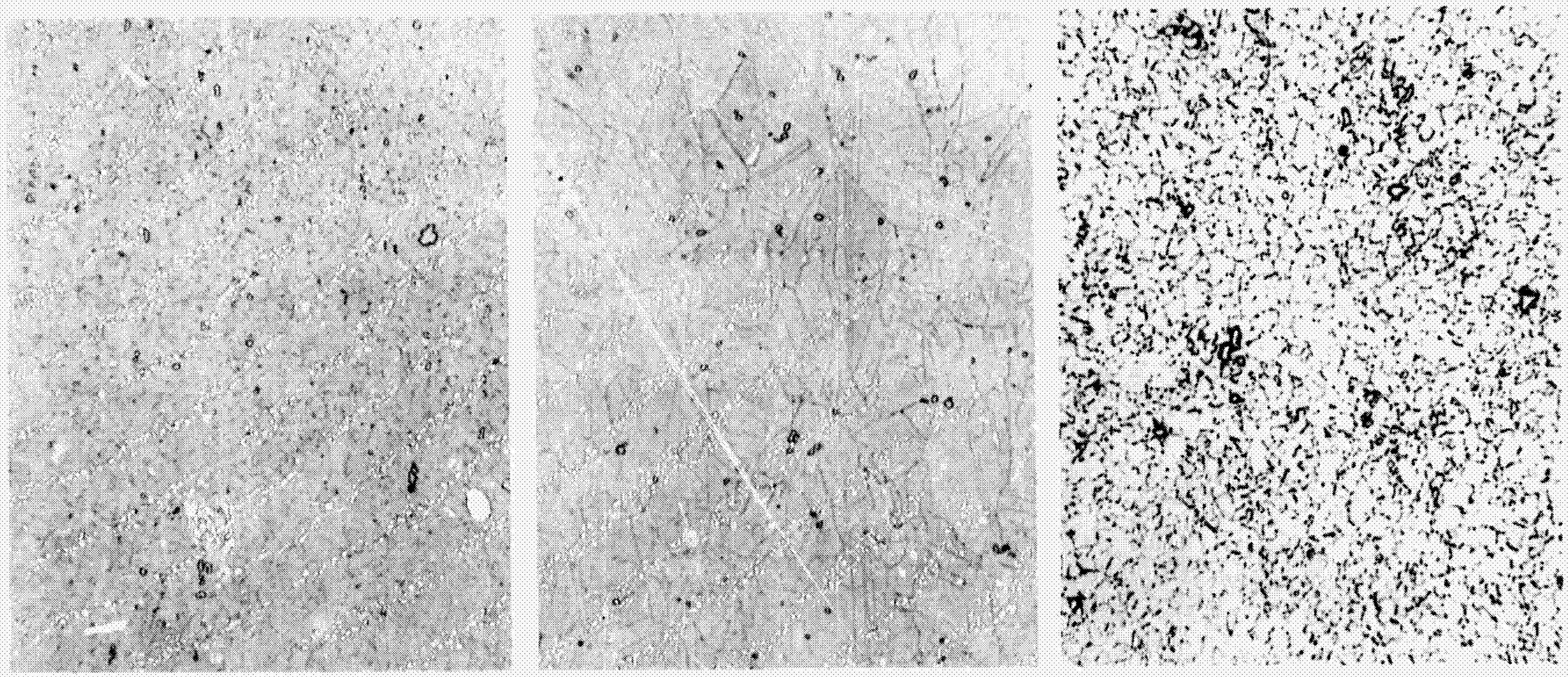

Plate   Forging   Rolled Bar

Figure 10. Photomicrographs of Transverse Sections of Inconel 718 in the 1725 F, 1325-1150 F Heat Treatment Condition. Etchant: 92 HCl, 3 HNO_3, 1/2 H_2SO_4 (200x)

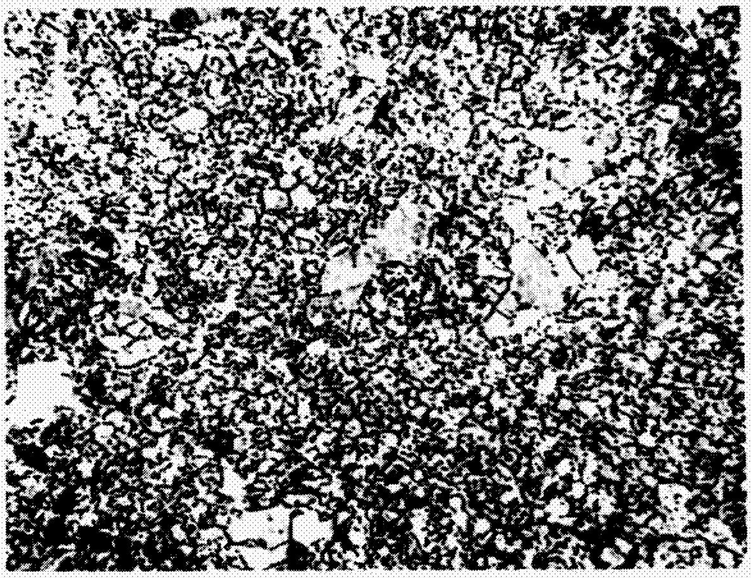

200x

Transverse Cross Section

200x

Longitudinal Cross Section

Figure 11. Photomicrographs of Inconel 718 Rolled Bar in the 1725 F, 1500-1200 F Heat Treatment Condition. Etchant: 92 HCl, 7 HNO_3, 1/2 H_2SO_4

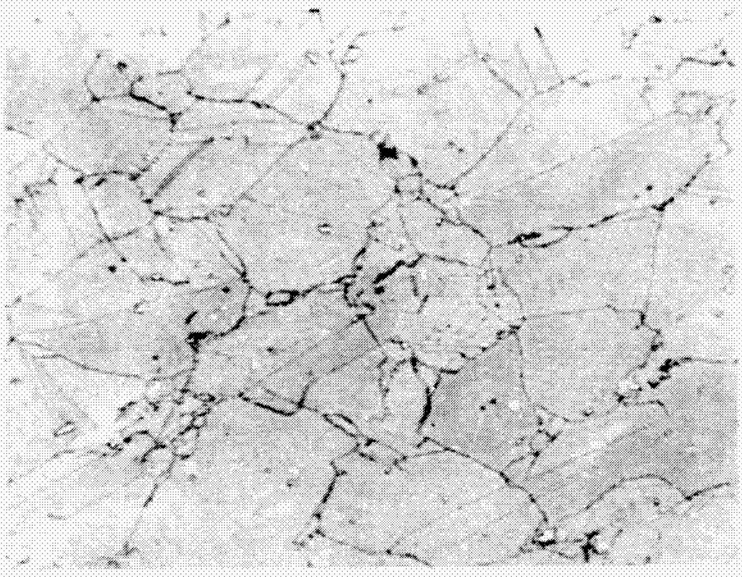

200x

Forging

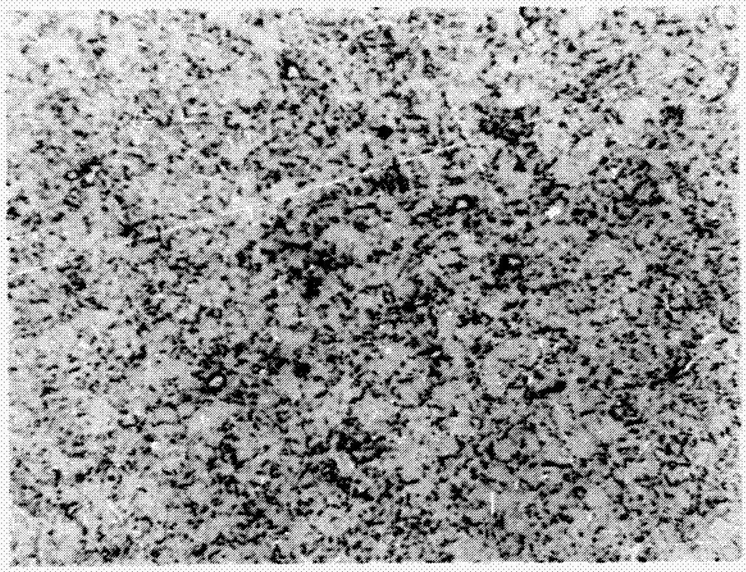

200x

Plate

Figure 12. Photomicrographs of Transverse Sections of Inconel 718 Forging and Plate in the 1725 F, 1500-1200 F Heat Treatment Condition. Etchant: 92 HCl, 3 HNO_3, 1/2 H_2SO_4

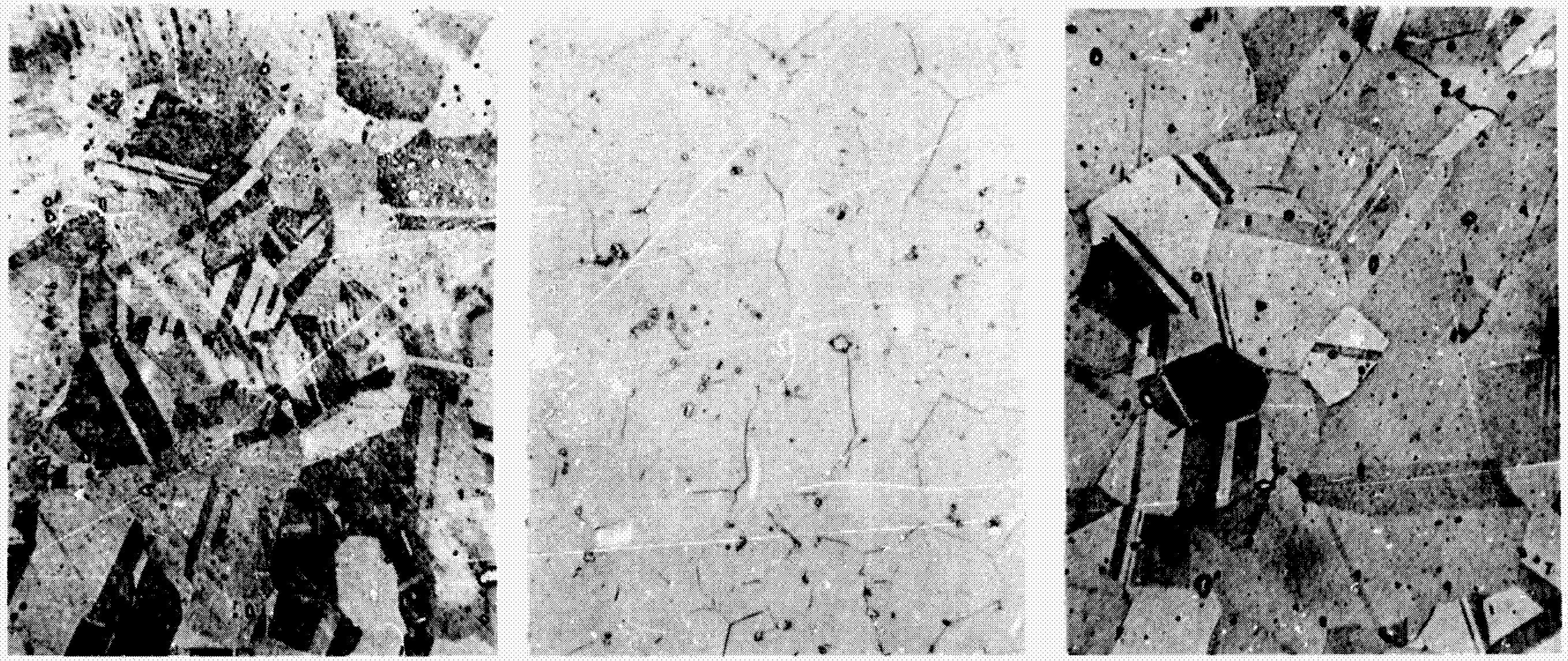

Plate Forging Rolled Bar

Figure 13. Photomicrographs of Transverse Sections of Inconel 718 in the 1950 F, 1400-1200 F Heat Treatment Condition Etchant: 92 HCl, 3 HNO_3, 1/2 H_2SO_4 (200x)

Electron micrographs of the bar, forging, and plate are shown in Fig. 14 for the 1750 F annealed, as received condition, in Fig. 15 for the 1725 F, 1325-1150 F heat treatment condition, in Fig. 16 for the 1725 F, 1500-1200 F heat treatment condition, and in Fig. 17 for the 1925 F, 1400-1200 F heat treatment condition. All of the electron micrographs are of transverse sections.

A second phase is evident in the 1750 F anneal, as received condition, and this phase appears essentially unchanged in amount and appearance when the rolled bar, forging and plate were subsequently heat treated at 1725, 1325-1150 F. This phase (or phases) has not yet been identified, but is believed to be either the A_2B Laves phase or the orthorhombic Ni_3Cb phase with the latter believed to be most likely.

The work of Eiselstein (Ref. 14) provides indirect evidence that the unidentified phase may be the Laves phase. Eiselstein developed a phase diagram which indicates that the Laves phase is stable for the 5 percent Cb + Ta composition in Inconel 718 at temperatures below 1900 F, and will go into solution above that temperature. He developed a TTT diagram for Inconel 718, which was annealed at 2100 F (1 hour) and water quenched, which indicated that the Laves phase would form after a one-hour aging treatment at 1700-1800 F, but that the Ni_3Cb phase would begin to form only after 5 hours at 1700-1800 F. Eiselstein also presented a TTT diagram for Inconel 718, which was solution annealed at 1700 F for two hours, which indicates that the Ni_3Cb phase would begin to form only after 5 to 10 hours at temperatures between 1500 and 1650 F and does not form in 10 hours at 1700 F. Unfortunately, Laves phase formation was not included in

Rolled
Bar

Forging

Plate

Figure 14. Electron Micrographs of Inconel 718 in the 1750 Annealed, as Received Condition. Etchant: 92 HCl, 3 HNO_3, 1/2 H_2SO_4 (3000x)

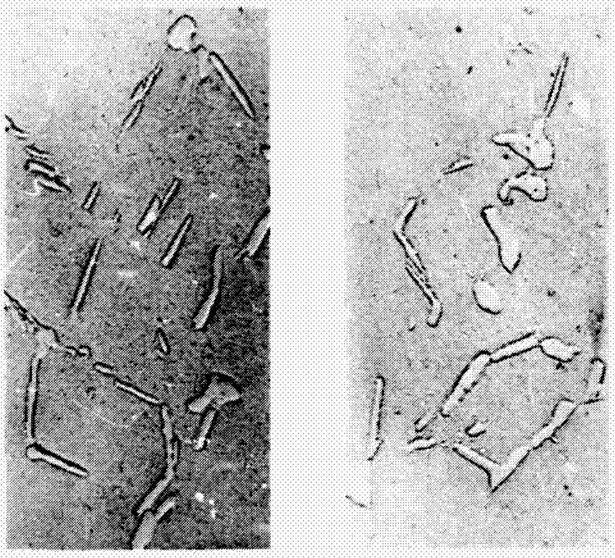

Rolled
Bar

Forging

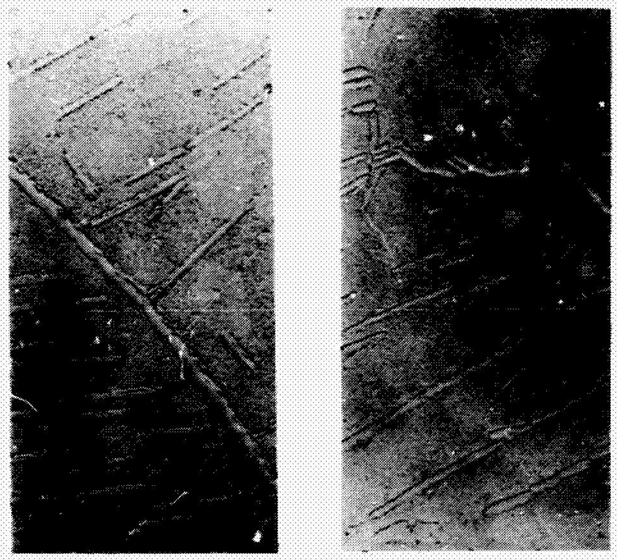

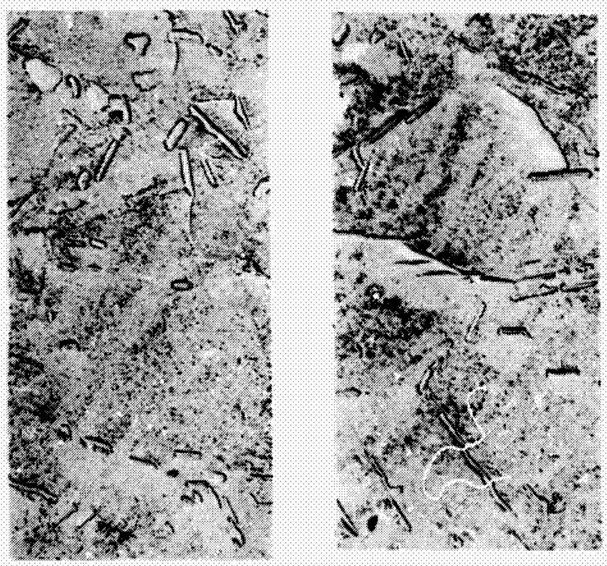

Plate

Figure 15. Electron Micrographs of Inconel 718 in the 1725 F, 1325-1150 F Heat Treatment Condition. Etchant: 92 HCl, 3 HNO_3, 1/2 H_2SO_4 (3000x)

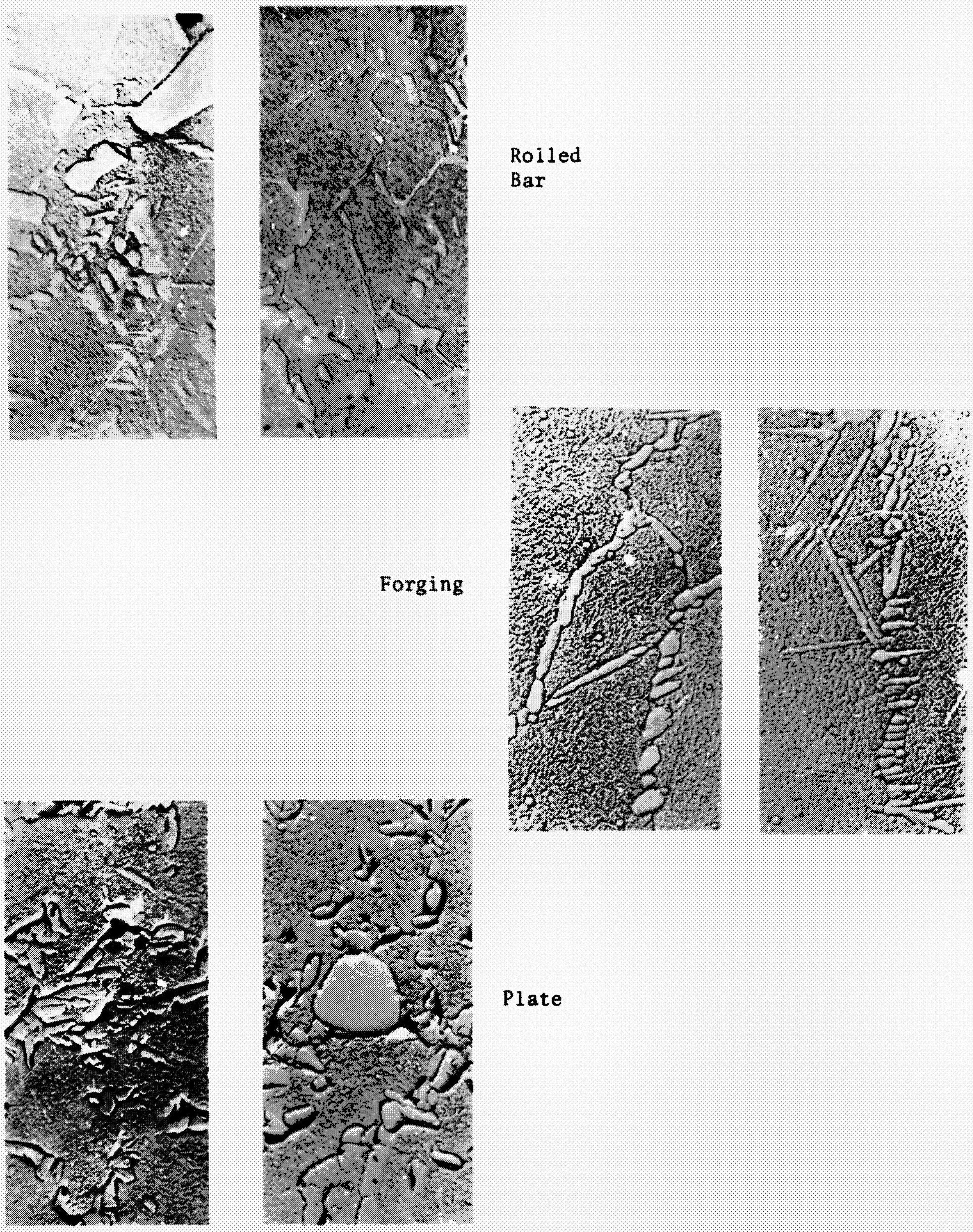

Figure 16. Electron Micrographs of Inconel 718 in the 1725 F, 1500 - 1200 F Heat Treatment Condition. Etchants: 92 HCl, 3 HNO_3, 1/2 H_2SO_4 (3000x)

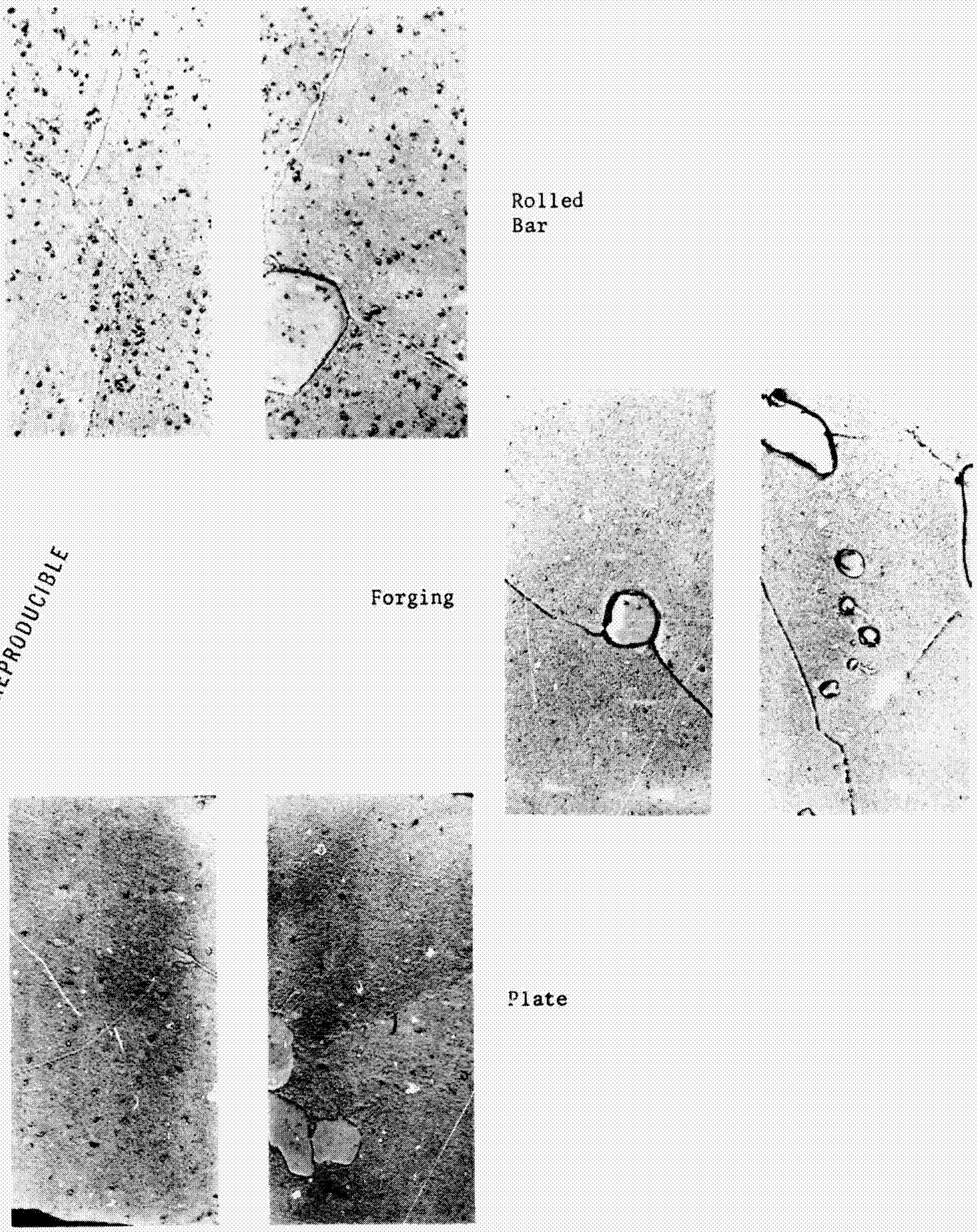

Figure 17. Electron Micrographs of Inconel 718 in the 1925 F, 1400 - 1200 F Heat Treatment Condition. Etchant: 92 HCl, 3 HNO_3, 1/2 H_2SO_4 (3000x)

this TTT diagram. There is no indication from these two TTT diagrams that the Ni_3Cb phase would form during the 1750 F, 1 hour anneal given the as-received Inconel 718 in this program, but there is some indication that the Laves phase would form during this anneal. Finally, Eiselstein indicated that the Laves phase appears as a flat, irregular precipitate while the Ni_3Cb phase typically appears as a needle-shaped precipitate in a Widmänstatten pattern.

Evidence that the second phase in Fig. 14 and 15 is Ni_3Cb come from Muzyka and Maniar (Ref. 15). They annealed Inconel 718 for 1 hour at various temperatures between 1725 and 1850 F followed by a 1325-1150 F aging treatment. The resulting microstructures appear similar to those shown in Fig. 14 and 15. Muzyka and Maniar used selected area electron diffraction and identified a precipitate similar to the one in Fig. 14 and 15 as being Ni_3Cb. They made no mention of the Laves phase and it is presumed that the Laves phase was not present or was there to a much smaller extent than the Ni_3Cb phase.

Tentatively, the phase in question is assumed to be the orthorombic Ni_3Cb phase and it will be so identified for the remainder of the discussion. Work is continuing to positively identify this phase.

Examination of Fig. 14 and 15 shows that the Ni_3Cb was somewhat discontinuous in the rolled bar, nearly continuous in the forging, and is dispersed in the plate. Thus, the as-receive[illegible] on of the: (a) rolled bar is duplex with somewhat discontinuous Ni_3[illegible], ([illegible] forging is large grained with nearly continuous Ni_3Cb and (c) pla[illegible] is fine grained with discontinuous Ni_3Cb.

During the 1325-1150 F aging treatment, coherent precipitates of γ' and γ" form throughout the structure and are not resolved at the magnifications used. Thus, the microstructures appear about the same in the 1725 F, 1325-1150 F condition as in the 1750 F annealed, as-received condition.

Figure 16 shows the electron microscopy of the bar, forging, and plate in the 1725 F, 1500-1200 F heat treatment condition. Overaging caused coarsening and loss of coherency of the γ' and γ" precipitates, and these phases are resolved in the electron micrographs shown in Fig. 16. Coarsening of the Ni_3Cb phase in all three electron micrographs is also evident.

Figure 17 shows the electron micrographs for the 1925 F, 1400-1200 F heat treatment condition. Recrystallization, grain growth, and dissolution occurred during the heat treatment, and the resulting microstructures of the bar, forging, and plate are all virtually the same. Figure 17 shows that the Ni_3Cb went into solution during the 1925 F solution anneal. A thin, intergranular, carbide film together with isolated carbide particles formed during the heat treatment.

Solution of the Ni_3Cb phase is consistent with Muzyka and Maniar (Ref. 15) who showed that the phase they identified as Ni_3Cb disappeared completely during a 1900 F anneal. Both Muzyka and Maniar (Ref. 15) and Eiselstein (Ref. 14) showed that a carbide film formed during solution annealing at 1900 F and at 1300-1500 F. On the other hand, Eiselstein (Ref. 14) showed that the carbide film would not form during aging after a 1700 F solution anneal.

The microstructures of the weld and heat affected zones of the 1/2 in. plate weldments are shown in Figure 18 for the 1725 F, 1325-1150 F heat treatment condition, in Figure 19 for the 1725 F, 1500-1200 F heat treatment condition and in Figure 20 for the 1925 F, 1400-1200 F heat treatment condition. A dendritic, cored structure is evident in the weld when in the 1725 F, 1325-1150 F and 1725 F, 1500-1200 F heat treatment conditions. The microstructures of the weld in the 1925 F, 1400-1200 F heat treatment condition appears similar to that for the parent metal but with somewhat smaller grain size and remnants of dendritic segregation.

The electron micrographs of the weld metal with the 1725, 1325-1150 F and 1725, 1500-1200 heat treatments show an almost continuous array of the phase assumed to be Ni_3Cb. This phase can also be seen in the electron micrographs of the heat-affected-zone of specimens with these same heat treatments and it is coarser and more continuous than in the parent metal. The heat-affected-zone also contained Ni_3Cb needles in the typical Widmänstatten pattern.

Electron micrographs of parent metal, weld metal, and heat-affected-zone all appear similar for weld specimens with the 1925, 1400-1200 F heat treatment. Intergranular carbide films and isolated carbide particles can be seen.

The characteristic differences, discussed above, among the microstructures of the Inconel 718 rolled bar, forging, and plate with the various heat treatments can be related, at least qualitatively, to the degree of embrittlement by the high-pressure hydrogen environment. First, it should be noted that electron fractography has corroborated for these specimens the previous findings (Ref. 4) that the fracture of Inconel 718, as well as other nickel-base alloys, in high-pressure hydrogen is intergranular in the hydrogen affected region.

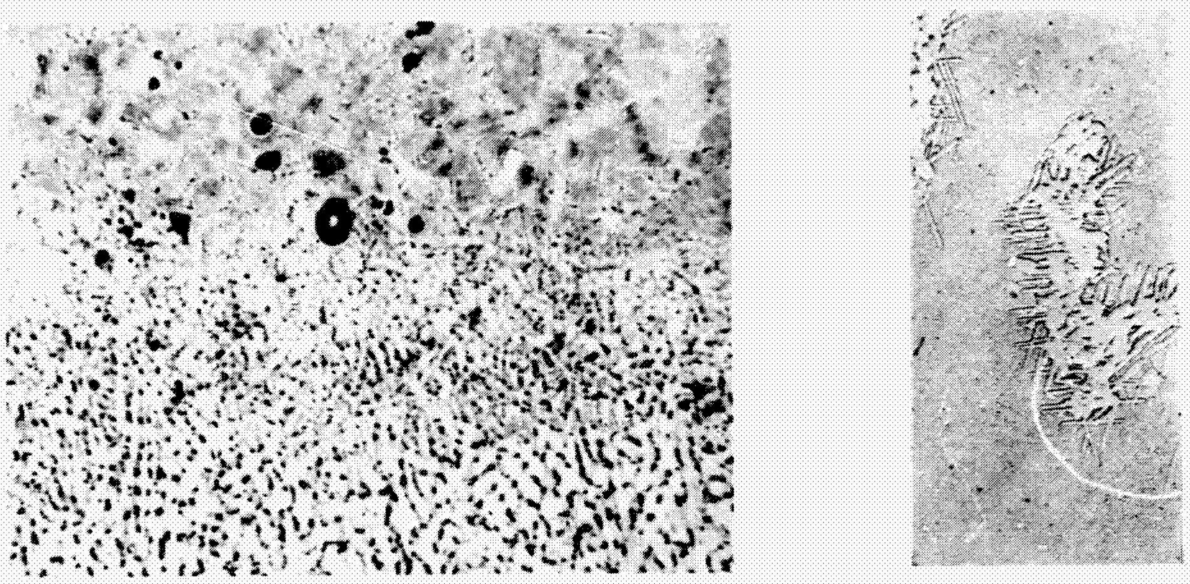

200x 3000x

Heat Affected Zone

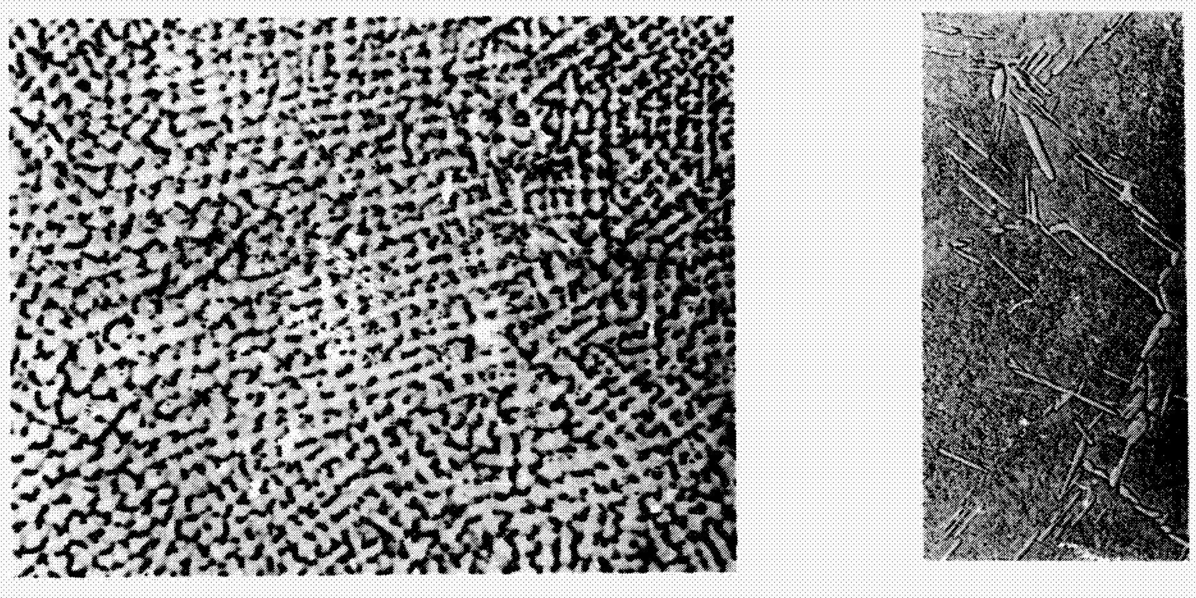

200x 3000x

Weld Metal

Figure 18. Optical and Electron Micrographs of Welded Inconel 718 Plate in the 1725 F, 1325 - 1150 F Heat Treatment Condition. Etchant: 92 HCl, 3 HNO_3, 1/2 H_2SO_4

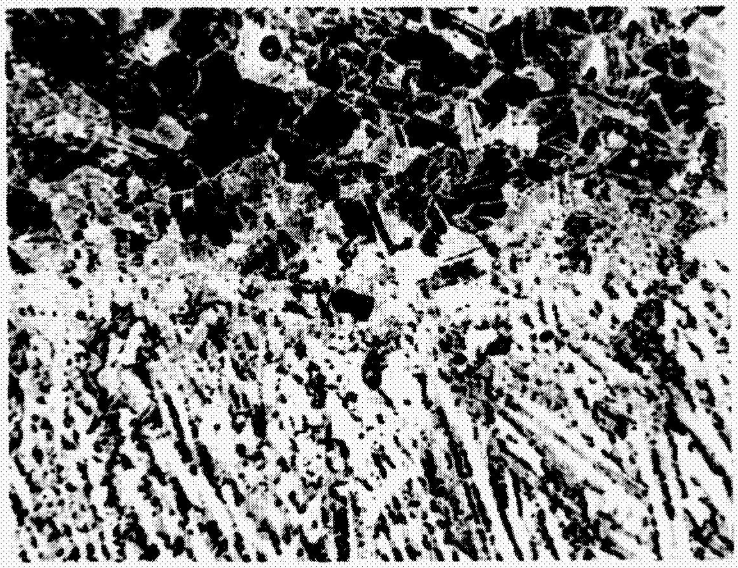

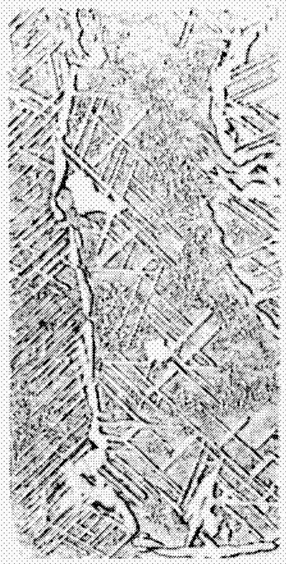

200x 3000x

Heat-Affected Zone

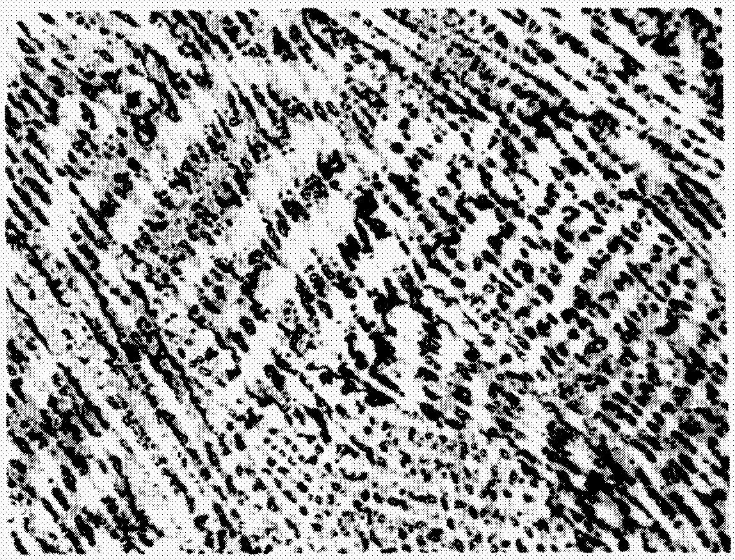

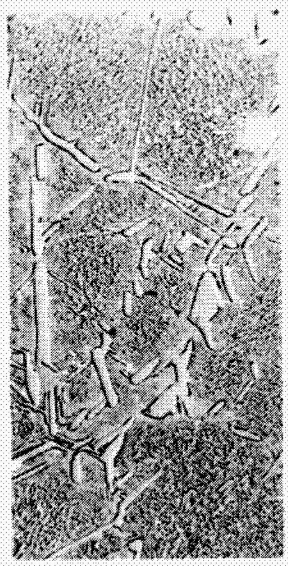

200x 3000x

Weld Metal

Figure 19. Optical and Electron Micrographs of Welded Inconel 718 Plate in the 1725 F, 1500-1200F Heat Treatment Condition. Etchant: 92 HCl, 3 HNO_3, 1/2 H_2SO_4

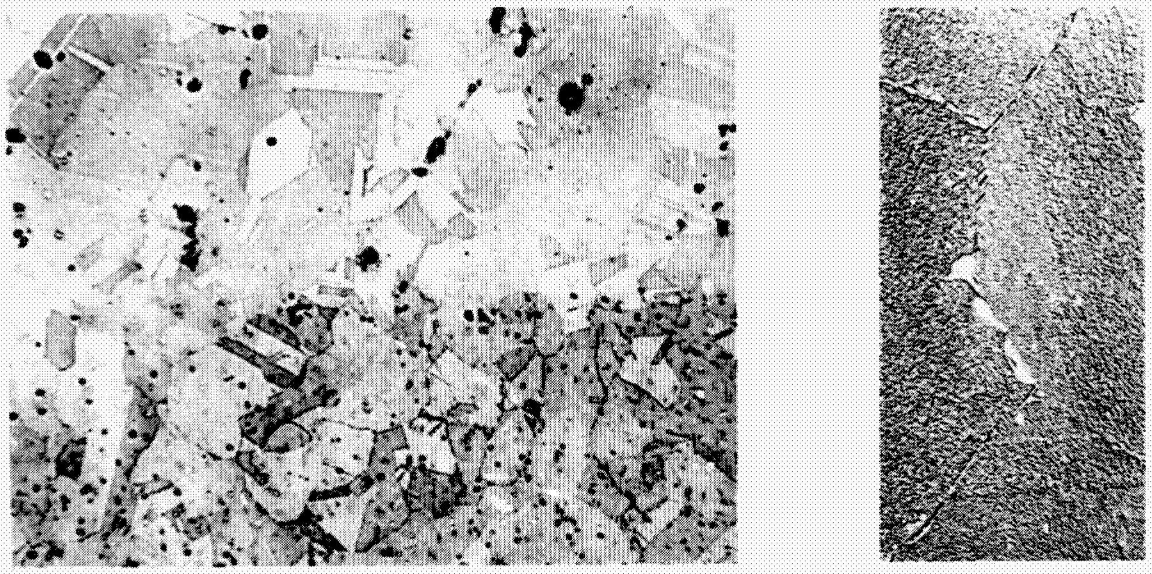

200x 3000x

Heat-Affected Zone

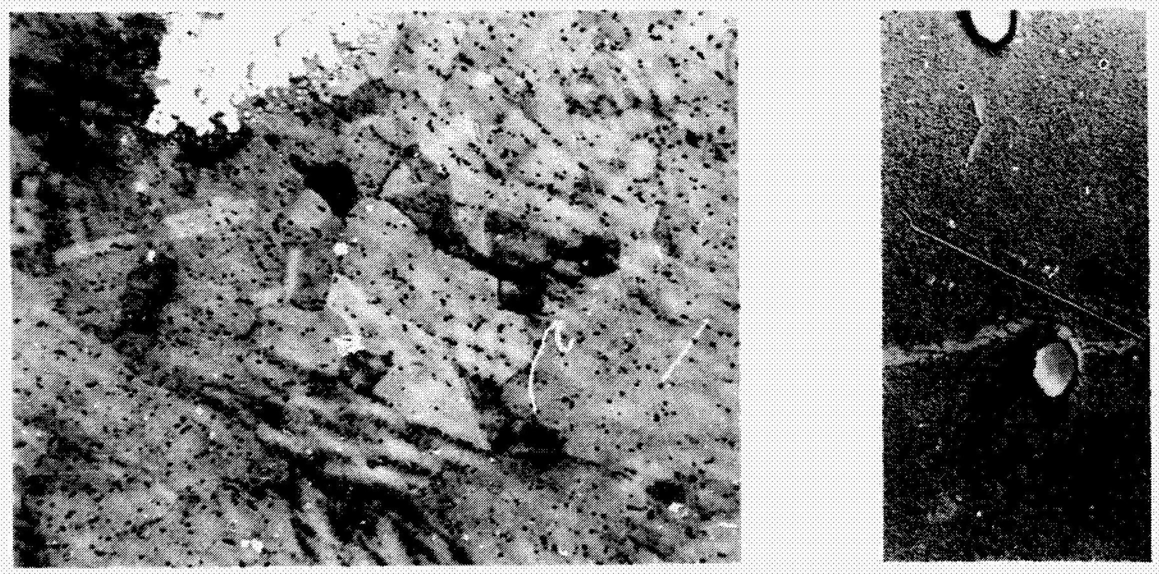

200x 3000x

Weld Metal

Figure 20. Optical and Electron Micrographs of Welded Inconel 718 Plate in the 1925 F, 1400 - 1200 F Heat Treatment Condition. Etchant: 92 HCl, 3 HNO_3, 1/2 H_2SO_4

The least embrittled microstructure, i.e., the plate with the 1725 F, 1325-1150 F heat treatment, was fine grained with discontinuous particles of the phase tentatively identified as Ni_3Cb. The most embrittled microstructure, i.e., the rolled bar and forging with the 1725 F, 1325-1150 F heat treatment, was either relatively large grained or a duplex structure of small and large grains with, in both cases, semi-continuous Ni_3Cb in the structure. The 1925, 1400-1200 F heat treatment resulted in a large grain size, the elimination of Ni_3Cb, the presence of carbide particles and intermetallic films and intermediate embrittlement for the rolled bar, the forging, and the plate. The 1725 F, 1500-1200 F overaging heat treatment coarsened the Ni_3Cb and the age hardening precipitate but did not significantly change embrittlement from that for the 1725, 1325-1150 F heat treatment. This lack of sensitivity of embrittlement to overaging indicates that the degree of hydrogen environment embrittlement is not strongly influenced by the age hardening precipitate size, morphology, or coherency.

It thus appears that the least embrittled microstructure is one which is fine grained with dispersed Ni_3Cb. A fine grained structure can be achieved only by severe working of the ingot and is not always feasible in large forgings. It is not clear which is the more important, dispersed Ni_3Cb or fine grain size. Removal of the Ni_3Cb phase by the 1925 F, 1400-1200 F heat treatment decreased embrittlement of the relatively large grained material. Increasing the grain size while removing the Ni_3Cb phase increased embrittlement of the fine grained material. On this basis, the optimum heat treatment may be the lowest time-temperature anneal to place the Ni_3Cb into solution and avoid grain growth. To determine this, tests are planned on each material solution annealed at 1875 F for 10 minutes and aged at 1400-1200 F. Tests are also planned on Inconel 718 annealed at 1875 F for 10 minutes without subsequent aging to determine the degree of embrittlement of as-annealed Inconel 718.

Associating hydrogen-environment embrittlement with Ni_3Cb does have the probl[illegible] other nickel-base alloys, such as René 41 and Waspalloy, which do [illegible] umbium, are also severely embrittled by hydrogen environ- [illegible]

TENSILE PROPERTIES OF ALLOYS IN HYDROGEN ENVIRONMENTS

The average tensile properties of Inconel 625, AISI Type 321 stainless steel, Ti-5Al-2.5Sn ELI, and OFHC copper tested in air, 5,000 psi helium, and 5,000 psi hydrogen are given in Table 7. The data for individual specimens are presented in Appendix A. As has been found in previous programs, none of the materials experienced any decrease in yield strength due to the hydrogen environment.

For Inconel 625, the ductility of unnotched specimens was considerably reduced and the strength and ductility of notched specimens was moderately reduced in 5,000 psi hydrogen compared to 5,000 psi helium at room temperature. Even the ultimate strength of the unnotched specimens was somewhat reduced in hydrogen at room temperature. The reduction of notch strength of Inconel 625 by 5,000 psi hydrogen is similar to that found for the more moderately embrittled conditions of Inconel 718 even though Inconel 625 is not as strong an alloy. Generally, everything else being equal, the stronger the alloy, the greater the susceptibility to hydrogen environment embrittlement. The reduction of ductility of Inconel 625 by hydrogen at room temperature was quite severe although considerable ductility was still present. The unnotched Inconel 625 specimens tested in hydrogen at room temperature contained surface cracks in the necked down region which were rather large and deep, similar to those that have been observed on steels such as ASTM A-302. The effect of 5,000 psi hydrogen on the tensile properties of Inconel 625 at -200 F was insignificant and no surface cracking was observed at this temperature.

For AISI 321 stainless steel, the strength and ductility of notched specimens was slightly reduced by 5,000 psi hydrogen compared to 5,000 psi helium

TABLE 7

AVERAGE TENSILE PROPERTIES OF INCONEL 625, AISI TYPE 321 STAINLESS STEEL, Ti-5Al-2.5Sn ELI, & OFHC COPPER IN VARIOUS ENVIRONMENTS

Material	Specimen Type	Environment			Test Results				
					Strength			Ductility	
		Temp. F	Type	Pressure psig	Yield KSI	Ultimate KSI	Strength Ratio H_2/He	Reduction of Area %	Elongation %
Inconel 625	UN	Rm	Air	0	94	144	--	54	50
	UN	Rm	Helium	5000	92	144	--	50	55
	UN	Rm	Hydrogen	5000	87	129	0.90	18	20
	N*	Rm	Helium	5000	-	208	--	9.4	-
	N	Rm	Hydrogen	5000	-	158	0.76	4.6	-
	UN	-200	Helium	5000	103	164	--	52	45
	UN	-200	Hydrogen	5000	101	162	--	48	43
	N	-200	Helium	5000	-	212	--	[illegible]	-
	N	-200	Hydrogen	5000	-	221	--	6.9	-
AISI 321 SS	UN	Rm	Air	0	32	87	--	71	77
	UN	Rm	Helium	5000	29	84	--	66	63
	UN	Rm	Hydrogen	5000	37	86	--	60	64
	N	Rm	Helium	5000	-	113	--	6.4	-
	N	Rm	Hydrogen	5000	-	99	0.88	2.3	-
	UN	-200	Helium	5000		124		67	48
	UN	-200	Hydrogen	5000		122		56	43
	N	-200	Helium	5000	-	143	--	12	-
	N	-200	Hydrogen	5000	-	141	--	12	-

TABLE 7

(CONTINUED)

		Environment			Test Results				
					Strength			Ductility	
Material	Specimen Type	Temp. F	Type	Pressure psig	Yield KSI	Ultimate KSI	Strength Ratio H_2/He	Reduction of Area %	Elonga-tion %
Ti-5Al-2.5Sn ELI	UN	Rm	Air	0	114	119	--	31	18
	UN	-200	Helium	5000	-	151	--	26	14
	UN	-200	Hydrogen	5000	107	149	--	30	9
	N	-200	Helium	5000	-	228	--	1.7	-
	N	-200	Hydrogen	5000	-	227	--	1.3	-
OFHC Copper	UN	Rm	Air	0	17	28	--	84	57
	UN	Rm	Helium	5000	12	28	--	85	63
	UN	Rm	Hydrogen	5000	11	27	--	84	65
	N	Rm	Helium	5000	-	43	--	23	-
	N	Rm	Hydrogen	5000	-	42	--	25	-
	N	-200	Helium	5000	-	41	--	29	-
	N	-200	Hydrogen	5000	-	44	--	24	-

*$K_t \simeq 8.7$ for all notched specimens

at room temperature. At -200 F, the properties of notched AISI stainless steel specimens were essentially unaffected by hydrogen. For unnotched AISI 321 stainless steel specimens, the reduction of area was decreased very slightly by hydrogen at room temperature but to a somewhat greater extent at -200 F. The unnotched AISI 321 stainless steel specimens tested in hydrogen contained surface cracks. At room temperature, numerous, small surface cracks formed over the entire reduced section, while at -200 F, larger surface cracks formed but were restricted mainly to the necked-down region. The fact that larger cracks formed at -200 F could account for the somewhat greater decrease in the reduction of area by hydrogen at -200 F than at room temperature. The behavior of the AISI 321 stainless steel in hydrogen is similar to that observed for other stainless steels, e.g., AISI 304, which tend to form martensite during deformation. The effects of hydrogen environments on these stainless steels has been attributed to cracking in the martensite in the hydrogen environment (Ref. 4 and 5).

In a previous program (Ref. 4), it was found that the N_{H_2}/N_{He} ratio for the Ti-5Al-2.5Sn ELI alloy was approximately 0.8 for pressures of 10,000 psi. However, tests were performed only at room temperature. The results in Table 7 show that this alloy was essentially unaffected by 5,000 psi hydrogen at -200 F. No surface cracks were observed in specimens tested in hydrogen.

The results in Table 7 show that OFHC copper was essentially unaffected by 5,000 psi hydrogen both at room temperature and -200 F. No surface cracks were formed.

THRESHOLD STRESS INTENSITY OF ALLOYS IN HYDROGEN ENVIRONMENTS

The results of the fracture toughness measurements on modified WOL specimens of various alloys in 5,000 psi hydrogen and 5,000 psi helium at room temperature are tabulated in Table 8. For most tests, the specimens were loaded to somewhat above the 5 percent secant offset which is considered in ASTM standards (Ref. 16) as the stress intensity at which unstable crack growth occurs during continuous loading. This stress intensity is designated K_{Ic} providing plane strain requirements are met. In order for a K_{Ic} value to be valid, the following test requirements must be met for the modified WOL specimen: (a) the load rate must be such that the rate of increase of the stress intensity is between 30 and 150 KSI $\sqrt{\text{in.}}$/min., (b) the change from linearity of the load versus deflection curve must be sufficiently sharp in the region between 0.8 and 1.0 of the 5 percent secant offset, (c) the specimen thickness and crack length must be greater than $2.5\left(\frac{K_{Ic}}{\sigma_{YS}}\right)^2$, and (d) the maximum deviation of the crack length must be within 5 percent of the average crack length. No special effort was made to load the specimens at a rate within the range required for a valid K_{Ic} value, however, most of the tests in air and helium environments met this requirement. On the other hand, the rate of loading in hydrogen was usually very slow so that the minimum stresses at which crack growth occurs would not be greatly exceeded. Table 9 lists the maximum stress intensities which meet the $2.5\left(\frac{K_I}{\sigma_{YS}}\right)^2$ requirement for the WOL specimen dimensions used for these tests. The 5 percent maximum deviation of crack length requirement was met for most of the tests. The actual crack length deviation is listed in Table 8 for those specimens for which the deviation exceeded 5 percent. Part of the reason the initial crack lengths deviated somewhat from a straight line was

TABLE 8

RESULTS OF FRACTURE TOUGHNESS MEASUREMENTS AT ROOM TEMPERATURE ON MODIFIED WOL SPECIMENS OF VARIOUS ALLOYS IN 5000 PSI HYDROGEN AND HELIUM ENVIRONMENTS

Material	Specimen No.	Environment	K_{Ic}: K_Q[c] KSI ($\sqrt{in.}$)	K_{Ic} Meets ASTM Standards: $2.5\left(\frac{K}{\sigma_{YS}}\right)^2$	K_{Ic} Meets ASTM Standards: 5% Secant Require.	K_{Ic} Meets ASTM Standards: Crack Uniformity[a]	K_{max} KSI ($\sqrt{in.}$)	K_{TH}: KSI ($\sqrt{in.}$)	K_{TH}: Time Held Under Load Hrs.	K_{TH} Meets ASTM Standards: $2.5\left(\frac{K_{TH}}{\sigma_{YS}}\right)^2$	K_{TH} Meets ASTM Standards: Crack Uniformity[a]	Comments
Inconel 718	A7	Air (1 atm)	75	yes	yes	yes	75	≥66[b]	19	yes	-	Pop-in
1725,	A2	He	68	yes	yes	yes	68	55	64	yes	yes	Pop-in
1325-1150 F[c]	A3	H_2	-	-	-	yes	32			yes	-	Specimen failed during hold period.
	A4	H_2	-	-	-	9.1	25			yes	-	Specimen failed during hold period.
	A5	H_2	-	-	-	yes	24	21	7.5	yes	22.4	Crack arrest determined by backing off of load.
Inconel 718 1925,	B2	He	105	marginal	no	yes	112	≥97[b]	17	marginal	-	Pop-in occurred after the 5% secant intersect.
1400-1200 F	B3	H_2	-	-	-	yes	64	50	8	yes	5.5	Crack arrest determined by backing off of load.
Inconel 625	2	He	63	no	yes	9.0	70	-	-	-	-	No crack growth
	3	He	90	no	yes	yes	90	-	40	no	-	No crack growth
	1[d]	H_2	49	yes	yes	yes	-	56	17	no	-	Crack branched and did not propagate

TABLE 8

(CONTINUED)

Material	Specimen No.	Environment	K_{Ic}: K_θ[c] KSI ($\sqrt{in.}$)	K_{Ic} Meets ASTM Standards: $2.5\left(\frac{K_\theta}{\sigma_{YS}}\right)^2$	K_{Ic} Meets ASTM Standards: 5% Secant Require.	K_{Ic} Meets ASTM Standards: Crack Uniformity[a]	K_{max} KSI ($\sqrt{in.}$)	K_{TH}: KSI ($\sqrt{in.}$)	K_{TH}: Time Held Under Load Hrs.	K_{TH} Meets ASTM Standards: $2.5\left(\frac{K_{TH}}{\sigma_{YS}}\right)^2$	K_{TH} Meets ASTM Standards: Crack Uniformity[a]	Comments
AISI 321 S.S.	1	He	30	no	yes	6.1	37	35	17	no	-	
	3[e]	H_2	27	no	yes	yes	29	28	1.5	no	11.0	
A-286 S.S.	4	He	126	no	no	yes	145	-	19.5	no	yes	No crack growth.
	3	H_2	-	-	no	yes	109	-	16	no	yes	No crack growth.
Ti-5Al-2.5Sn	2	He	76	marginal	-	yes	76	>50[b]	65	yes	15.0	Pop-in occurred with a questionable load-deflection trace.
	3	H_2	-	yes	yes	yes	51	38	40	yes	7.5	
2219 T-87 Al Alloy	3	He	20	yes	yes	yes	20	-	-	-	-	Specimen failed during loading.
	4	H_2	23	yes	yes	6.0	27	>16[b]	64	yes	15	
	6	H_2	27	yes	yes	yes	28	>20[b]	15	yes	6.1	

TABLE 8

(CONCLUDED)

Material	Specimen No.	Environment	K_{Ic}: K_θ[c] KSI ($\sqrt{in.}$)	K_{Ic} Meets ASTM Standards: $\left(\frac{K_\theta}{\sigma_{YS}}\right)^2$ 2.5	K_{Ic} Meets ASTM Standards: 5% Secant Require.	K_{Ic} Meets ASTM Standards: Crack Uniformity[a]	K_{max} KSI ($\sqrt{in.}$)	K_{TH}: KSI ($\sqrt{in.}$)	K_{TH}: Time Held Under Load Hrs.	K_{TH} Meets ASTM Standards: $\left(\frac{K_{TH}}{\sigma_{YS}}\right)^2$ 2.5	K_{TH} Meets ASTM Standards: Crack Uniformity[2]	Comments
OFHC Copper	2	He	20	no	yes	yes	22	-	18	no	-	No crack growth, plastic deformation only. (Both Specimens)
	4	He	16	no	yes	yes	17	-	15	no	-	
	3	H_2	17	no	yes	yes	18	-	18	no	-	No crack growth, plastic deformation only.

(a) Yes indicates deviation is less than 5%, or number indicates % deviation.

(b) Sustained crack growth occurred but final crack length could not be identified. K_{TH} calculations based on crack length at beginning of test.

(c) K_θ = Conditional value of fracture toughness from test data.

(d) Specimen was initially stressed to 56.1 KSI $\sqrt{in.}$ (no crack growth). Unloaded and exposed to air. Reloaded in H_2 and final arrest occurred at 126 KSI $\sqrt{in.}$

(e) Specimen was unloaded, exposed to air and reloaded in increments to a maximum stress intensity of 71.7. Crack growth occurred with each increment held but crack extension stopped soon afterwards. Final crack extension 0.121 inch plus considerable plastic deformation.

TABLE 9

MAXIMUM STRESS INTENSITIES AT WHICH PLANE STRAIN EXISTS
FOR WOL SPECIMENS USED FOR THESE TESTS

Material	Yield Strength KSI	K_I Max. For Plane Strain
Inconel 718	162	100
Inconel 625	94	58
AISI 321 S. S.	32	20
A-286	113	70
Ti-5Al-2.5Sn ELI	119	73
2219-T87 Al Alloy	57	35
OFHC Copper	17	10

that the fabricator inadvertently did not in most cases use electrical discharge machining (EDM) for machining the straight notched specimens, although the specimen design called for EDM machining of the notch. Novak (Ref. 17) has found that EDM machining of the straight notched specimens is usually necessary for obtaining a straight fatigue precrack. There was a tendency for the crack arrest to occur at greater crack lengths in the specimen center than at the edges which may be indicative of greater environmental effects at the plane strain locations at the specimen center than at the edges.

Table 8 includes the K_{Ic} measured from the tests, the stress intensity, K_{max}, at which loading was stopped and the crack allowed to propagate until arrested at K_{TH}, and pertinent information as to whether ASTM plane strain requirements were met.

Inconel 718

The Inconel 718, WOL specimens were fabricated from the same rolled bar used in Phase 1. The fracture toughness measurements on Inconel 718 indicated considerable differences in fracture toughness between specimens given the 1725, 1325-1150 F heat treatment and specimens given the 1925, 1400-1200 F heat treatment. Pop-in (sudden load decrease during loading) occurred in the air and helium environments and thus there is comparatively little uncertainty of the K_{Ic} values. The plane strain fracture toughness, K_{Ic}, for the 1925, 1400-1200 F condition was 105 KSI$\sqrt{in.}$ compared to 68-75 KSI $\sqrt{in.}$ for the specimens in the 1725, 1325-1150 F condition. There was a small amount of crack growth following pop-in of the Inconel 718 specimen #7 (1725, 1325-1150 F) tested in air, and specimen #2 (1925 F, 1400-1200 F) tested in 5,000 psi helium. Unfortunately, the post fatigue marking was inadequate to discern the final crack length and the K_{TH} value was therefore calculated from the crack length at the beginning of the test. On this basis, K_{TH} for Inconel 718 in the 1725 F, 1325-1150 F condition was between 66 and 75 KSI $\sqrt{in.}$ in air and 55 KSI $\sqrt{in.}$ in 5,000 psi helium, and K_{TH} in 5,000 psi helium for Inconel 718 in the 1925 F, 1400-1200 F condition was between 97 and 112 KSI $\sqrt{in.}$

Initial tests conducted in 5,000 psi hydrogen on Inconel 718 specimens in the 1725 F, 1325-1150 F heat treatment condition resulted in complete fracture of the specimens although the maximum stress intensities to which the specimens were loaded were comparatively low. A threshold value was then obtained on specimen #5 by bracketing the load at which crack growth was noted rather than by crack arrest. The K_{TH} value obtained by this method was 21 KSI $\sqrt{in.}$ which is virtually the same (22 KSI $\sqrt{in.}$) as obtained by Lorenz (Ref. 9) on Inconel 718 plate in the same heat treatment condition and tested in 5,200 psi hydrogen.

The threshold stress intensity in 5,000 psi hydrogen for Inconel 718 in the 1925 F, 1400-1200 F condition was also measured by bracketing rather than by arrest. The K_{TH} obtained was 50 KSI $\sqrt{in.}$ which was over twice the measured K_{TH} for the 1725 F, 1325-1150 F condition.

Significant crack opening displacement was noted during crack growth of the specimens which failed completely in 5,000 psi hydrogen. Thus, the load was not decreasing sufficiently rapidly for crack arrest because of elastic deformation of the loading fixture. To rectify this, the loading bridge and stub shaft were redesigned to decrease elastic deflection while the specimen was loaded. The final designs of these components are those shown in Figs. 4 and 7.

Inconel 625

The K_{Ic} values calculated, using the 5 percent secant method, for Inconel 625 specimens tested in 5,000 psi helium were 63 and 90 KSI $\sqrt{in.}$ These values are not valid because plane strain conditions were not met for these tests and there was no indication of sustained crack growth in these specimens when they were held at 70 and 90 KSI $\sqrt{in.}$ The load vs. deflection curve for the Inconel 625 specimen tested in 5,000 psi hydrogen crossed the 5 percent secant line at 49 KSI $\sqrt{in.}$ Holding this specimen at a stress intensity of 56 KSI $\sqrt{in.}$ for 17 hours did not result in any indication of further crack extension. The specimen was exposed to air and then later reloaded in 5,000 psi hydrogen in increments up to a stress intensity of 126 KSI $\sqrt{in.}$ With each loading increment above approximately 80 KSI $\sqrt{in.}$ stress intensity, there was a small indication of crack extension, but significant crack growth did not occur even at 126 KSI $\sqrt{in.}$ Post examination showed that crack branching had occurred at an angle to the plane of the fatigue crack. Thus, there was no meaningful crack arrest data obtained. It is possible, however, that there was initial crack extension at 49 KSI $\sqrt{in.}$ which corresponded to the 5 percent secant intersect.

The crack branching in Inconel 625 is characteristic (Ref. 4) of alloys which are severely embrittled during tensile testing in high pressure hydrogen environments. The branching causes the cracks to change direction toward the tensile axis, which decreases the stress intensity at the crack tip and causes the crack to cease propagating. Branching also occurred on tensile specimens of alloys which were extremely embrittled by high-pressure hydrogen. The cracks, however, continued to propagate perpendicular to the tensile axis despite crack branching.

AISI 321 Stainless Steel

Plane strain conditions were not obtained with the AISI 321 stainless steel specimens in either 5,000 psi helium or 5,000 psi hydrogen. The K_{TH} of 35 KSI $\sqrt{in.}$ in 5,000 psi helium is probably not meaningful because crack blunting occurred instead of crack extension as there was no measured change in crack depth during the test.

The first indication of sustained flaw growth in 5000 psi hydrogen occurred at 28 KSI $\sqrt{in.}$ Subsequent reloading in increments up to 72 KSI $\sqrt{in.}$ resulted in crack extension with each loading increment and the crack arrested each time within a few minutes even though the loads had not decreased to the previous arrest values. Post examination showed that the specimen had deformed plastically (over 0.2 inch crack opening displacement) and the crack front appeared rounded. There was considerable surface cracking along the side grooves just ahead of the precrack. Examination of the specimen after fatigue marking and fracture indicated that considerable crack growth (0.121 inch) had occurred during the test. The sustained crack growth region was very smooth with an almost polished appearance and contained no branching as observed on the Inconel 625 specimen tested in hydrogen. It was therefore evident that the crack extended a certain amount with each load increase and then blunted by rounding of the crack front without secondary cracking or branching. Thus although sustained flaw growth did occur, the stress intensity at crack arrest was a function of the stress intensity at which it was loaded. Therefore there does not appear to be a K_{TH} value as normally conceived for AISI 321 in 5000 psi hydrogen.

Crack blunting of the AISI 321 stainless steel specimen in 5000 psi hydrogen was similar (Ref. 4) to the rounded surface cracks that formed on AISI 304L stainless steel specimens tensile tested in 10,000 psi hydrogen. Benson, Dann and Roberts (Ref. 5) suggested from electron fractography examination that the hydrogen initiated microcracks formed at strain induced martensitic areas in the AISI 304L stainless steel. Blunting evidently occurs in the surrounding ductile austenitic matrix.

A-286 Stainless Steel

The fracture toughness of A-286 stainless steel appears to be very high. The stress intensity at the 5 percent secant intercept was 126 KSI $\sqrt{in.}$ in 5,000 psi helium. No sustained flaw growth was evident while the specimens were held at 145 KSI $\sqrt{in.}$ in 5,000 psi helium and 109 KSI $\sqrt{in.}$ in 5,000 psi hydrogen.

Ti-5Al-2.5Sn ELI

Sustained flaw growth occurred for the Ti-5Al-2.5Sn ELI specimens in 5,000 psi hydrogen and 5,000 psi helium. The specimen tested in helium was loaded to 76 KSI $\sqrt{in.}$, which corresponded to K_{Ic} in helium, and sustained crack growth occurred, and arrested at a stress intensity > 50 KSI $\sqrt{in.}$ The post fatigue mark could not be resolved so the threshold stress intensity was calculated using the crack length at the beginning of the test.

A threshold value of 38 KSI $\sqrt{in.}$ was measured by the bracketing method for the test conducted in 5,000 psi hydrogen. This value is higher than the threshold stress intensity of 21.5 KSI $\sqrt{in.}$ obtained by Bixler (Ref. 18) for Ti-5Al-2.5Sn ELI from measurements conducted at room temperature in 1,400 psi hydrogen. The hydrogen affected region of the fracture in hydrogen was very dark and in some regions almost black. This dark texture is usually indicative of extensive secondary cracking, but could also be due to formation of a hydride phase.

2219-T87 Al Alloy

The plane strain fracture toughness (K_{Ic}) ranged between 20 and 27 KSI $\sqrt{in.}$ for the 2219-T87 Al alloy tested in 5,000 psi hydrogen and 5,000 psi helium.

The specimen tested in 5000 psi helium failed after reaching a maximum stress intensity of about 20 KSI $\sqrt{in}$. Sustained crack growth and crack arrest occurred during the tests conducted in 5000 psi hydrogen but the K_{TH} value could only be estimated as >16 or 19 KSI $\sqrt{in}$. because the post fatigue marking could not be resolved. Although the fracture toughness data obtained on this alloy were very qualitative, there does not appear to be a reduction of fracture toughness because of the 5000 psi hydrogen environment.

OFHC Copper

Crack growth in the OFHC copper specimens did not occur during the tests in either 5000 psi hydrogen or 5000 psi helium. Loading above the 5 percent secant offset caused bending without crack extension for the specimen tested in both environments.

Additional fracture toughness tests are being performed for each of the above materials in 5000 psi helium and 5000 psi hydrogen at room temperature. Tests will also be performed on each material in these environments at -200 F.

SUMMARY AND CONCLUSIONS

In order to correlate the results of the three different phases, the results will be summarized by material.

INCONEL 718

The degree of hydrogen-environment embrittlement of Inconel 718, as measured by the reductio of notch tensile strength at room temperature in 5000 psi hydrogen, was found to be a function of both forming operation and heat treatment. Of the three forms of Inconel 718 tested, i.e., rolled bar, forging and plate, the plate had the lowest and most consistent hydrogen-environment embrittlement for the three heat treatment conditions tested. The least hydrogen embrittlement, i.e., the highest N_{H_2}/N_{He} ratio occurred with the 1725, 1325-1150 F and 1725, 1500-1200 F heat treatments of the plate. On the other hand, the greatest embrittlement resulted from the 1725, 1325-1150 F heat treatment of the rolled bar and forging. Of the three heat treatments, the 1925, 1400-1200 F heat treatment gave the most consistent results. For all three forms, rolled bar, forging and plate, the 1925, 1400-1200 F heat treatment resulted in the highest notch strength both in helium and hydrogen.

Fracture toughness tests were conducted on the rolled bar in the 1725, 1325-1150 F and 1925, 1400-1200 F heat treatment conditions. The highest fracture toughness values in both helium and hydrogen resulted from the 1925, 1400-1200 F heat treatment. The notch strength and fracture toughness were nearly as high in 5000 psi hydrogen for the 1925, 1400-1200 F heat treatment condition as were these properties in 5,000 psi helium for the

1725, 1325-1150 F heat treatment condition. The superior notch and fracture toughness properties in hydrogen of the 1925, 1400-1200 F condition may be related to the higher notch ductility and thus lower notch sensitivity of Inconel 718 in this condition compared to the 1725, 1325-1150 F heat treatment condition.

The characteristic differences among the microstructures of the Inconel 718 rolled bar, forging, and plate with various heat treatments can be related, at least qualitatively to the degree of embrittlement. The most embrittled Inconel 718 microstructure was one which was coarse grained and contained an almost continuous network of a phase tentatively identified as Ni_3Cb. The least embrittled microstructure was one which was fine grained with the Ni_3Cb being very disperse. Removal of the Ni_3Cb phase by the 1925, 1400-1200 F heat treatment decreased embrittlement of the relatively large grained material. Increasing the grain size of the fine grained material by the 1925, 1400-1200 F heat treatment increased embrittlement even though the Ni_3Cb phase was eliminated.

With respect to hydrogen environment embrittlement of the welded Inconel 718 specimens, the weld metal with the 1925, 1400-1200 F heat treatment was the most severely embrittled condition. As with the parent metal, the notch strength in helium of both the weld metal and heat-affected-zone was higher with the 1925, 1400-1200 F heat treatment than with the other two heat treatments. However, the degree of hydrogen environment embrittlement of the weld metal was large enough for the 1925, 1400-1200 F heat treatment that the notch strength in hydrogen was somewhat lower with that heat treatment than with the 1725, 1325-1150 F heat treatment. Therefore, the fine dendritic weld structure of the 1725, 1325-1150 F condition was less embrittled by the hydrogen environments than the equiaxed recrystallized structure of the 1925, 1400-1200 F heat treatment.

For the parent metal and weld metal, the 1725, 1500-1200 F overaging heat treatment did not significantly change embrittlement from that for the 1725, 1325-1150 F heat treatment. This lack of sensitivity of embrittlement to overaging indicates that the degree of hydrogen environment embrittlement is not strongly influenced by the age hardening precipitate size, morphology, or coherency.

INCONEL 625

The ductility of unnotched Inconel 625 specimens was considerably reduced, and the strength and ductility of notched specimens was moderately reduced in 5,000 psi hydrogen compared to 5,000 psi helium at room temperature. Even the ultimate strength of unnotched specimens was somewhat reduced in hydrogen at room temperature. The unnotched specimens contained surface cracks in the necked-down region which were rather large and deep. The effect of 5,000 psi hydrogen on the tensile properties of Inconel 625 at -200 F was insignificant, and no surface cracking was observed at this temperature.

The fracture toughness measurement in high-pressure hydrogen was affected by branching of the crack at an angle to the crack plane. This decreased the stress intensity at the crack tip and caused the crack to cease to propagate. The stress intensity at crack arrest was, therefore, not measured. There is some evidence, however, that initial crack growth occurred at about 49 KSI $\sqrt{\text{in.}}$ stress intensity.

Crack branching was probably an important factor determining the tensile as well as fracture toughness properties of Inconel 625 in hydrogen. The fact that there were several fairly large surface cracks formed on the unnotched specimens is an indication of crack branching. Crack branching in tensile specimens can cause the crack to change direction toward the tensile axis, reduce the stress at the crack tip, cause the crack to cease propagating, and give other surface cracks an opportunity to form.

AISI 321 STAINLESS STEEL

The strength and ductility of the notched AISI 321 stainless steel specimens were slightly reduced by 5,000 psi hydrogen at room temperature and were essentially unaffected by hydrogen at -200 F. The reduction of area of the unnotched specimens was decreased slightly by hydrogen at room temperature and to a somewhat greater extent at -200 F. Surface cracks formed in unnotched specimens. They were numerous and small and were observed along the whole reduced section at room temperature and were somewhat larger and limited to the necked-down region at -200 F. The larger surface cracks at -200 F may account for the larger decrease in the reduction of area at -200 F than at room temperature.

Considerable plastic blunting at the crack front accompanied crack growth in the WOL specimens of AISI 321 stainless steel tested in 5,000 psi hydrogen. With each increase of load between 28 and 72 KSI $\sqrt{\text{in.}}$, there was crack extension which arrested each time within a few minutes, but the load did not decrease to the previous arrest values. Therefore, there does not appear to be a K_{TH} value, as normally conceived, for AISI 321 stainless steel in 5,000 psi hydrogen at room temperature. Plastic blunting of the crack correlates with rounding of surface cracks such as observed on 304 stainless steel specimens tensile tested in high-pressure hydrogen environments.

Ti-5Al-2.5Sn ELI

The tensile properties at -200 F of Ti-5Al-2.5Sn ELI alloy were not reduced by 5,000 psi hydrogen. In a previous program (Ref. 4), it was found that N_{H_2}/N_{He} was approximately 0.8 in 10,000 psi hydrogen at room temperature.

Sustained flaw growth occurred for Ti-5Al-2.5Sn ELI specimens in 5,000 psi hydrogen and 5,000 psi helium at room temperature. A threshold value of 38 KSI $\sqrt{in.}$, compared to a K_{Ic} of 76 in 5,000 psi helium, was measured for a test conducted in 5,000 psi hydrogen.

A-286 STAINLESS STEEL, 2219-T87 ALUMINUM ALLOY AND OFHC COPPER

The tensile properties of OFHC copper were essentially unaffected by 5,000 psi hydrogen both at room temperature and -200 F. The room temperature fracture toughness measurements conducted on A-286 stainless steel, 2219 -T87 aluminum alloy and OFHC copper indicated that the fracture toughness of these alloys were not reduced by the 5,000 psi hydrogen environment. Although plane strain conditions were not obtained on A-286 stainless steel, the fracture toughness of this alloy appears to be very high (> 126 KSI $\sqrt{in.}$).

CRACK PROPAGATION IN HYDROGEN

The manner in which cracks propagate in high-pressure hydrogen environments has been recognized (Ref. 4) as an important factor determining the mechanical properties of metals in hydrogen environments. The results of this program have given added emphasis to the importance of this factor.

In previous work (Ref. 4), it was shown that those specimens which were tensile tested in 10,000 psi hydrogen, but the tensile properties of which were not affected by the hydrogen environments, did not contain surface cracks. A-286 stainless steel, OFHC copper, and the aluminum alloys were in this category, and it appears from the current program that sustained flaw growth of these alloys (including the 2219-T87 aluminum alloy) is not influenced by the 5,000 psi hydrogen environment.

When surface cracks form, blunting can occur by either rounding of the surface cracks or by crack branching. The least embrittled of those metals that form surface cracks were those (Ref. 4) in which the surface cracks blunted by rounding. AISI 321 stainless steel is in this category. Crack rounding caused numerous small surface cracks to form, caused a small decrease of notch strength and inhibited sustained crack growth during fracture toughness measurements.

Branching of the cracks appears to occur in the remainder of the metals embrittled by hydrogen. For the lesser embrittled of this group, branching causes the cracks to change crack propagation direction, and the cracks cease to propagate. The depth that the cracks grow prior to changing direction determines to a large degree the reduction of tensile properties. Inconel 625 is evidently in this category, and there was an indication of flaw growth in hydrogen at a considerably lower stress intensity than in the helium environment. However, because of crack branching, significant sustained flaw growth did not occur even with increasing applied stress intensity above that at which flaw growth was first noted.

Crack branching also occurs for the most embrittled metals. The branching, however, does not appear to substantially affect crack propagation because the cracks continue propagating in a straight line despite branching, and generally only one surface crack forms on unnotched specimens and this crack propagates to failure. There is a considerable decrease of fracture toughness of these metals and K_{TH} in hydrogen is appreciably lower than in air and helium environments. Fracture toughness data for the extremely embrittled metals, can be treated in the normal manner. That is, flaw growth will occur in practice at stress intensities above the measured K_{TH} obtained by tests conducted in the service environment.

Utilization of fracture mechanics data for materials such as 321 stainless steel and Inconel 625 is more difficult. There is a critical stress intensity at which flaw growth will occur and in thin sections this amount of flaw growth could be critical. Fatigue loading may resharpen the flaw in the direction normal to the applied load and an increment of sustained flaw growth may be repeated.

It would be dangerous to depend on crack rounding or branching to inhibit crack growth in practice since they may be a function of orientation, flaw depth, stress conditions (plane stress or plane strain) in front of the crack tip, and probably other factors.

REFERENCES

1. Walter, R. J. and W. T. Chandler, "Effect of High-Pressure Hydrogen on Metals," paper presented at 1968 Materials Engineering Congress, Detroit, Michigan, October 1968. ASM Report No. D8-14.2, ASM Report System, Metals Park, Ohio.

2. Walter, R. J. and W. T. Chandler, "Effect of High-Pressure Hydrogen on Storage Vessel Materials," paper presented at WESTEC Conference, Los Angeles, California, March 1968. ASM Report No. W8-2.4, ASM Report System, Metals Park, Ohio.

3. Steinman, J. B., H. C. Van Ness, and G. S. Ansell, "The Effect of High-Pressure Hydrogen Upon the Notch Tensile Strength and Fracture Mode of 4140 Steel," Welding Journal, May 1965, pp. 221s-224s.

4. Walter, R. J. and W. T. Chandler, "Effects of High-Pressure Hydrogen on Metals at Ambient Temperatures," Final Report on Task 7 of NASA Contract NAS8-19, Rocketdyne, a Division of North American Rockwell Corporation, Canoga Park, California, Report No. R-7780-1, -2, -3, February 1969.

5. Benson, R. B., Jr., R. K. Dann, and L. W. Roberts, Jr., "Hydrogen Embrittlement of Stainless Steel," Trans. AIME, 242, p. 2199, 1968.

6. Hofmann, V. W. and W. Rauls, "Ductility of Steel Under the Influence of External High-Pressure Hydrogen, Welding Journal, May 1965, pp. 225s-230s.

7. Cavett, R. H. and H. C. Van Ness, "Embrittlement of Steel by High Pressure Hydrogen Gas, Welding Journal, July 1963, pp. 316s-319s.

8. Vennett, R. M. and G. S. Ansell, "The Effect of High-Pressure Hydrogen Upon the Tensile Properties and Fracture Behavior of 304L Stainless Steel," Trans. ASM, 60, p. 242, 1967.

9. Lorenz, P. M., "Effect of Pressurized Hydrogen Upon Inconel 718 and 2219 Aluminum," paper presented at WESTEC Conference, Los Angeles, California, March 1969, ASM Report No. W9-13.2, ASM Report System, Metals Park, Ohio.

10. Walter, R. J. and W. T. Chandler, "Effect of Hydrogen Environments on Inconel 718 and Ti-6Al-4V (STA)," paper presented at AIME Meeting, Las Vegas, Nevada, 11-14 May 1970.

11. Vennett, R. M. and G. S. Ansell, "A Study of Gaseous Hydrogen Damage in Certain FCC Metals," Trans. Quart. ASM, 62, p. 1007, 1969.

12. Peterson, R. E., Stress Concentration Design Factors, John Wiley & Sons, New York, 1953.

13. Novak, S. R. and S. T. Rolfe, "Modified WOL Specimen for K_{ISCC} Environmental Testing," Journal of Materials, 4, No. 3, 1969, 701.

14. Eiselstein, H. L., "Metallurgy of a Columbium-Hardened Nickel-Chromium-Iron Alloy," from Advances in the Technology of Stainless Steels and Related Alloys, Special Technical Publication No. 369, American Society for Testing Materials, 1965.

15. Muzyka, D. R. and G. N. Maniar, "Effects of Solution Treating Temperature and Microstructure on the Properties of Hot Rolled 718 Alloy," Metals Engineering Quarterly, 9, No. 4, November 1969, 23.

16. "Tentative Method of Test for Plane-Strain Fracture Toughness of Metallic Materials," ASTM Standards, E399-70T, 1970, pp. 911-27.

17. Novak, S. R., Applied Research Laboratory, U. S. Steel Corporation, Monroeville, Pennsylvania, Personal Communication, 14 October 1970.

18. Bixler, W. D., "Flaw Growth of Inconel 718 and 5Al-2.5Sn (ELI) Titanium in a High-Purity Gaseous Hydrogen Environment," Boeing Document D180-10142-1, September 1970, prepared for Aerojet General Corporation, Sacramento, California, Contract L-80076, The Boeing Company, Seattle, Washington.

APPENDIX A

The following tables contain the data for the individual tensile tests performed under Phases I and II.

TABLE A-1

ROOM TEMPERATURE TENSILE PROPERTIES OF INCONEL 718 SPECIMENS FABRICATED FROM 1-1/4 IN. x 2-3/4 IN. ROLLED BAR SUPPLIED BY ALLVAK

Heat Treatment			Specimen			Environment		Test Results				
								Strength			Ductility	
Solution Temp. F	Aging Temps											
	First	Second	No.	Type	Stress Conc. Factor	Type	Pressure psig	Yield KSI	Ultimate KSI	Strength Ratio H_2/He	Reduction of Area	Percent Elongation
1725	1325	1150	IA-1	UN	-	Air	0	161	201	-	34	23
			IA-2	UN	-	Air	0	165	203	-	36	22
			IA-6	N	8.7	Helium	5000	-	284	-	2.8	-
			IA-7	N	8.7	Helium	5000	-	281	-	2.9	-
			IA-3	N	8.9	Hydrogen	5000	-	150	0.53	0.8	-
			IA-4	N	8.9	Hydrogen	5000	-	113	0.40	0.5	-
			IA-5	N	8.5	Hydrogen	5000	-	192	0.68	1.5	-
1925	1400	1200	IB-1	UN	-	Air	0	160	195	-	36	25
			IB-2	UN	-	Air	0	161	195	-	37	26
			IB-6	N	8.5	Helium	5000	-	322	-	4.6	-
			IB-7	N	8.9	Helium	5000	-	321	-	5.3	-
			IB-3	N	8.2	Hydrogen	5000	-	228	0.71	1.9	-
			IB-4	N	8.7	Hydrogen	5000	-	228	0.71	2.1	-
			IB-5	N	8.7	Hydrogen	5000	-	234	0.73	1.1	-
1725	1500	1200	IC-1	UN	-	Air	0	127	182	-	33	24
			IC-2	UN	-	Air	0	127	182	-	31	24
			IC-6	N	8.9	Helium	5000	-	245	-	2.9	-
			IC-7	N	8.7	Helium	5000	-	234	-	2.9	-
			IC-3	N	8.7	Hydrogen	5000	-	166	0.69	0.9	-
			IC-4	N	8.5	Hydrogen	5000	-	175	0.73	1.3	-
			IC-5	N	8.9	Hydrogen	5000	-	164	0.68	3.3	-

TABLE A-2

ROOM TEMPERATURE TENSILE PROPERTIES OF INCONEL 718 SPECIMENS FABRICATED FROM 1-1/2 IN. FORGING; SUPPLIED BY CARLTON FORGE, MILL SUPPLIER: SPECIAL METALS

Heat Treatment			Specimen			Environment		Test Results				
								Strength			Ductility	
Solution Temp. F	Aging Temps First	Aging Temps Second	No.	Type	Stress Conc. Factor	Type	Pressure psig	Yield KSI	Ultimate KSI	Strength Ratio H_2/He	Reduction of Area	Percent Elongation
1725	1325	1150	IG-1	UN	-	Air	0	154	199	-	29	22
			IG-2	UN	-	Air	0	164	197	-	32	21
			IG-6	N	8.7	Helium	5000	-	293	-	2.4	-
			IG-7	N	8.5	Helium	5000	-	286	-	3.5	-
			IG-3	N	8.3	Hydrogen	5000	-	180	0.62	1.3	-
			IG-4	N	8.9	Hydrogen	5000	-	159	0.55	0.9	-
			IG-5	N	8.3	Hydrogen	5000	-	172	0.59	1.1	-
1925	1400	1200	IH-1	UN	-	Air	0	170	200	-	42	26
			IH-2	UN	-	Air	0	168	196	-	39	26
			IH-6	N	8.0	Helium	5000	-	340	-	3.0	-
			IH-7	N	8.3	Helium	5000	-	338	-	6.2	-
			IH-3	N	8.9	Hydrogen	5000	-	250	0.74	1.3	-
			IH-4	N	8.7	Hydrogen	5000	-	259	0.76	2.2	-
			IH-5	N	8.3	Hydrogen	5000	-	265	0.78	2.0	-
1725	1500	1200	II-1	UN	-	Air	0	133	183	-	35	24
			II-2	UN	-	Air	0	115	173	-	34	26
			II-6	N	8.7	Helium	5000	-	248	-	1.9	-
			II-7	N	8.5	Helium	5000	-	258	-	2.5	-
			II-3	N	8.8	Hydrogen	5000	-	145	0.57	1.3	-
			II-4	N	8.5	Hydrogen	5000	-	136	0.54	1.0	-
			II-5	N	8.7	Hydrogen	5000	-	150	0.59	1.2	-

TABLE A-3

ROOM TEMPERATURE TENSILE PROPERTIES OF INCONEL 718 SPECIMENS FABRICATED FROM 1/2 IN. THICK PLATE SUPPLIED BY STELLITE DIV., CABOT CORP.

Heat Treatment			Specimen			Environment		Test Results				
								Strength			Ductility	
Solution Temp. F	Aging Temps First	Aging Temps Second	No.	Type	Stress Conc. Factor	Type	Pressure psig	Yield KSI	Ultimate KSI	Strength Ratio H_2/He	Percent Reduction of Area	Percent Elongation
1725	1325	1150	ID-1	UN	-	Air	0	160	206	-	36	22
			ID-2	UN	-	Air	0	158	204	-	36	23
			ID-6	N	8.0	Helium	5000	-	277	-	2.0	-
			ID-7	N	8.9	Helium	5000	-	296	-	4.0	-
			ID-3	N	8.7	Hydrogen	5000	-	257	0.89	2.4	-
			ID-4	N	8.4	Hydrogen	5000	-	233	0.81	2.0	-
			ID-5	N	8.3	Hydrogen	5000	-	249	0.87	1.7	-
1925	1400	1200	IE-1	UN	-	Air	0	163	204	-	37	25
			IE-2	UN	-	Air	0	170	203	-	39	24
			IE-6	N	8.7	Helium	5000	-	319	-	3.6	-
			IE-7	N	8.7	Helium	5000	-	321	-	3.8	-
			IE-5	N	8.7	Hydrogen	5000	-	248	0.78	2.9	-
			IE-3	N	8.3	Hydrogen	5000	-	246	0.77	2.1	-
			IE-4	N	8.5	Hydrogen	5000	-	248	0.78	2.0	-
1725	1500	1200	IF-1	UN	-	Air	0	133	188	-	36	23
			IF-2	UN	-	Air	0	133	189	-	33	23
			IF-6	N	8.7	Helium	5000	-	248	-	3.0	-
			IF-7	N	8.1	Helium	5000	-	254	-	2.3	-
			IF-3	N	8.9	Hydrogen	5000	-	216	0.86	2.0	-
			IF-4	N	8.1	Hydrogen	5000	-	219	0.87	1.5	-
			IF-5	N	8.3	Hydrogen	5000	-	216	0.86	2.9	-

TABLE A-4

ROOM TEMPERATURE TENSILE PROPERTIES OF WELDED SPECIMENS OF
INCONEL 718 1/2 IN. PLATE, 1725 F SOLUTION, 1325 F & 1150 F AGING TEMPERATURES

Specimen			Environment		Stress Conc. Factor	Test Results				
						Strength			Ductility	
No.	Type		Type	Pressure psig		Yield KSI	Ultimate KSI	Strength Ratio H_2/He	Percent Reduction of Area	Percent Elon-gation
IJW-11	UN	Weld	Air	0	-	154	185	-	1.5	6.3
IJW-12	UN	Weld	Air	0	-	146	161	-	9.2	3.4
IJW-1	N	Weld	Helium	5000	8.7	-	198	-	1.7	-
IJW-2	N	Weld	Helium	5000	8.7	-	213	-	1.0	-
IJW-3	N	Weld	Hydrogen	5000	8.7	-	167	0.81	1.1	-
IJW-4	N	Weld	Hydrogen	5000	8.9	-	165	0.80	0.8	-
IJW-5	N	Weld	Hydrogen	5000	8.9	-	159	0.76	1.1	-
IJW-6	N	HAZ	Helium	5000	8.3	-	289	-	2.6	-
IJW-10	N	HAZ	Helium	5000	8.1	-	242	-	0.9	-
IJW-7	N	HAZ	Hydrogen	5000	8.5	-	164	0.62	1.1	-
IJW-8	N	HAZ	Hydrogen	5000	8.5	-	176	0.66	0.4	-
IJW-9	N	HAZ	Hydrogen	5000	8.3	-	164	0.62	0.7	-

TABLE A-5

ROOM TEMPERATURE TENSILE PROPERTIES OF WELDED SPECIMENS OF
INCONEL 718 1/2 IN. PLATE, 1725 F SOLUTION, 1500 F & 1200 F AGING TEMPERATURES

Specimen			Environment		Stress Conc. Factor	Test Results				
						Strength			Ductility	
No.	Type		Type	Pressure psig		Yield KSI	Ultimate KSI	Strength Ratio H_2/He	Percent Reduction of Area	Percent Elon-gation
IIW-11	UN	Weld	Air	0	-	127	164	-	12	6.2
IIW-12	UN	Weld	Air	0	-	125	168	-	14	8.5
IIW-1	N	Weld	Helium	5000	8.9	-	186	-	2.1	-
IIW-2	N	Weld	Helium	5000	8.7	-	174	-	2.0	-
IIW-3*	N	Weld	Hydrogen	5000	8.7	-	-	-	-	-
IIW-4	N	Weld	Hydrogen	5000	8.9	-	145	0.81	0.8	-
IIW-5	N	Weld	Hydrogen	5000	8.7	-	135	0.75	0.4	-
IIW-6	N	HAZ	Helium	5000	8.7	-	209	-	1.3	-
IIW-7	N	HAZ	Helium	5000	8.3	-	195	-	1.5	-
IIW-8	N	HAZ	Hydrogen	5000	8.7	-	151	0.75	2.0	-
IIW-9	N	HAZ	Hydrogen	5000	8.5	-	149	0.74	0.5	-
IIW-10	N	HAZ	Hydrogen	5000	8.5	-	156	0.77	0.9	-

*Failed during pressurization.

TABLE A-6

ROOM TEMPERATURE TENSILE PROPERTIES OF WELDED SPECIMENS OF
INCONEL 718 1/2 IN. PLATE, 1925 F SOLUTION, 1400 F & 1200 F AGING TEMPERATURES

Specimen			Environment		Stress Conc. Factor	Test Results				
						Strength			Ductility	
No.	Type		Type	Pressure psig		Yield KSI	Ultimate KSI	Strength Ratio H_2/He	Percent Reduction of Area	Percent Elon-gation
IKW-11	UN	Weld	Air	0	-	166	199	-	19	11
IKW-12	UN	Weld	Air	0	-	164	198	-	26	15
IKW-1	N	Weld	Helium	5000	8.7	-	262	-	2.6	-
IKW-4	N	Weld	Helium	5000	8.7	-	274	-	2.5	-
IKW-2	N	Weld	Hydrogen	5000	8.7	-	148	0.55	0.8	-
IKW-3	N	Weld	Hydrogen	5000	8.7	-	175	0.65	0.9	-
IKW-5	N	Weld	Hydrogen	5000	8.9	-	131	0.49	0.7	-
IKW-6	N	HAZ	Helium	5000	8.1	-	310	-	5.0	-
IKW-7	N	HAZ	Helium	5000	8.9	-	292	-	2.6	-
IKW-8	N	HAZ	Hydrogen	5000	8.7	-	237	0.79	0.4	-
IKW-9	N	HAZ	Hydrogen	5000	8.7	-	181	0.60	0.8	-
IKW-10	N	HAZ	Hydrogen	5000	8.7	-	232	0.77	2.1	-

TABLE A-7

TENSILE PROPERTIES OF INCONEL 625 IN VARIOUS ENVIRONMENTS

Specimen			Environment			Test Results				
						Strength			Ductility	
No.	Type	Stress Conc. Factor	Type	Pressure psig	Temp. F	Yield KSI	Ultimate KSI	Strength Ratio H_2/He	Reduction of Area %	Elongation %
I-1	UN	-	Air	0	Rm	96	146	-	56	45
I-2	UN	-	Air	0	Rm	91	142	-	51	54
I-11	UN	-	Helium	5000	Rm	90	142	-	51	56
I-12	UN	-	Helium	5000	Rm	94	146	-	49	54
I-3	UN	-	Hydrogen	5000	Rm	86	126	0.88	18	21
I-4	UN	-	Hydrogen	5000	Rm	93	133	0.92	21	19
I-5	UN	-	Hydrogen	5000	Rm	82	128	0.89	16	19
I-21	N	8.7	Helium	5000	Rm	-	197	-	8.9	-
I-22	N	8.7	Helium	5000	Rm	-	219	-	9.8	-
I-13	N	8.9	Hydrogen	5000	Rm	-	161	0.77	3.9	-
I-14	N	8.9	Hydrogen	5000	Rm	-	154	0.74	5.0	-
I-15	N	8.7	Hydrogen	5000	Rm	-	160	0.77	5.0	-
I-6	UN	-	Helium	5000	-200	105	166	-	52	45
I-7	UN	-	Helium	5000	-200	101	162	-	51	44
I-8	UN	-	Hydrogen	5000	-200	102	162	-	48	40
I-9	UN	-	Hydrogen	5000	-200	95	152	-	47	42
I-10	UN	-	Hydrogen	5000	-200	106	172	-	49	48
I-16	N	8.7	Helium	5000	-200	-	217	-	8.0	-
I-17	N	8.9	Helium	5000	-200	-	206	-	8.2	-
I-18	N	8.9	Hydrogen	5000	-200	-	228	-	7.4	-
I-19	N	8.9	Hydrogen	5000	-200	-	215	-	6.7	-
I-20	N	8.9	Hydrogen	5000	-200	-	219	-	6.5	-

TABLE A-8

TENSILE PROPERTIES OF AISI TYPE 321 STAINLESS STEEL
IN VARIOUS ENVIRONMENTS

Specimen			Environment			Test Results				
						Strength			Ductility	
No.	Type	Stress Conc. Factor	Type	Pressure psig	Temp. F	Yield KSI	Ultimate KSI	Strength Ratio H_2/He	Reduction of Area %	Elongation %
S-1	UN	-	Air	0	Rm	32	87	-	71	77
S-2	UN	-	Air	0	Rm	31	87	-	70	77
S-11	UN	-	Helium	5000	Rm	28	85	-	65	62
S-12	[illegible]	-	Helium	5000	Rm	30	83	-	67	64
S-4	UN	-	Hydrogen	5000	Rm	36	86	-	59	63
S-6	UN	-	Hydrogen	5000	Rm	37	85	-	61	64
S-21	N	8.4	Helium	5000	Rm	-	111	-	6.3	-
S-22	N	8.7	Helium	5000	Rm	-	115	-	6.5	-
S-13*	N	8.7	Hydrogen	5000	Rm	-	101	0.89	1.2	-
S-14**	N	8.7	Hydrogen	5000	Rm	-	98	0.87	2.0	-
S-15	N	8.9	Hydrogen	5000	Rm	-	97	0.86	3.6	-
S-25	UN	-	Helium	5000	-200	-	120	-	67	45
S-29	UN	-	Helium	5000	-200	-	128	-	66	51
S-26	UN	-	Hydrogen	5000	-200	-	113	-	64	38
S-27***	UN	-	Hydrogen	5000	-200	-	118	-	53	39
S-28	UN	-	Hydrogen	5000	-200	-	134	-	51	51
S-16	N	8.5	Helium	5000	-200	-	142	-	14	-
S-17	N	8.7	Helium	5000	-200	-	143	-	10	-
S-18	N	8.7	Hydrogen	5000	-200	-	145	-	9.6	-
S-20	N	8.7	Hydrogen	5000	-200	-	141	-	14	-

*Specimen bent and straightened prior to testing.

**5000 psi hydrogen was established during test, but prior to plastic deformation.

***Leakage occurred near end of test and the final test temperature was -50 F.

TABLE A-9

TENSILE PROPERTIES OF Ti-5Al-2.5Sn ELI IN VARIOUS ENVIRONMENTS

Specimen			Environment			Test Results				
						Strength			Ductility	
No.	Type	Stress Conc. Factor	Type	Pressure psig	Temp. F	Yield KSI	Ultimate KSI	Strength Ratio H_2/He	Reduction of Area %	Elongation %
T-1	UN	-	Air	0	Rm	114	119	-	30	17
T-2	UN	-	Air	0	Rm	114	119	-	32	19
T-6	UN	-	Helium	5000	-200	-	152	-	26	11
T-7	UN	-	Helium	5000	-200	-	149	-	26	16
T-3	UN	-	Hydrogen	5000	-200	95	151	-	33	10
T-4	UN	-	Hydrogen	5000	-200	116	152	-	29	10
T-5	UN	-	Hydrogen	5000	-200	111	144	-	28	8
T-8	N	8.9	Helium	5000	-200	-	230	-	1.6	-
T-9	N	8.7	Helium	5000	-200	-	225	-	1.7	-
T-10	N	8.9	Hydrogen	5000	-200	-	228	-	1.4	-
T-11	N	8.7	Hydrogen	5000	-200	-	228	-	1.5	-
T-12	N	8.7	Hydrogen	5000	-200	-	226	-	0.9	-

TABLE A-10

TENSILE PROPERTIES OF OFHC COPPER IN VARIOUS ENVIRONMENTS

Specimen			Environment			Test Results				
						Strength			Ductility	
No.	Type	Stress Conc. Factor	Type	Pressure psig	Temp. F	Yield KSI	Ultimate KSI	Strength Ratio H_2/He	Reduction of Area %	Elongation %
C-1	UN	-	Air	0	Rm	15	28	-	84	61
C-2	UN	-	Air	0	Rm	18	28	-	83	53
C-11	UN	-	Helium	5000	Rm	11	28	-	81	62
C-12	UN	-	Helium	5000	Rm	12	27	-	88	63
C-3	UN	-	Hydrogen	5000	Rm	11	27	-	86	62
C-4	UN	-	Hydrogen	5000	Rm	11	27	-	83	65
C-5	UN	-	Hydrogen	5000	Rm	10	26	-	84	68
C-21	N	8.7	Helium	5000	Rm	-	44	-	25	-
C-22	N	8.8	Helium	5000	Rm	-	41	-	21	-
C-13	N	8.7	Hydrogen	5000	Rm	-	40	-	24	-
C-14	N	8.8	Hydrogen	5000	Rm	-	43	-	26	-
C-15	N	8.7	Hydrogen	5000	Rm	-	44	-	25	-
C-19	N	8.7	Helium	5000	-200	-	40	-	30	-
C-20	N	8.8	Helium	5000	-200	-	41	-	28	-
C-16	N	8.7	Hydrogen	5000	-200	-	41	-	30	-
C-17	N	8.6	Hydrogen	5000	-200	-	46	-	23	
C-18	N	8.7	Hydrogen	5000	-200	-	45	-	20	-

Unclassified

Security Classification

DOCUMENT CONTROL DATA - R & D

(Security classification of title, body of abstract and indexing annotation must be entered when the overall report is classified)

1. ORIGINATING ACTIVITY (Corporate author)

ROCKETDYNE
a division of North American Rockwell Corporation
6633 Canoga Avenue, Canoga Park, California 91304

2a. REPORT SECURITY CLASSIFICATION

Unclassified

2b. GROUP

3. REPORT TITLE

Influence of Gaseous Hydrogen on Metals

4. DESCRIPTIVE NOTES (Type of report and inclusive dates)

Interim

5. AUTHOR(S) (First name, middle initial, last name)

Robert J. Walter
Hoyt G. Hayes
Wilton T. Chandler

6. REPORT DATE	7a. TOTAL NO. OF PAGES	7b. NO. OF REFS
24 May 1971	98	18

8a. CONTRACT OR GRANT NO.	9a. ORIGINATOR'S REPORT NUMBER(S)
NAS8-25579	R-8719
b. PROJECT NO.	
c.	9b. OTHER REPORT NO(S) (Any other numbers that may be assigned this report)
d.	

10. DISTRIBUTION STATEMENT

11. SUPPLEMENTARY NOTES	12. SPONSORING MILITARY ACTIVITY

13. ABSTRACT

A program was performed to determine the gaseous hydrogen environment embrittlement of Inconel 718, Inconel 625, AISI 321 stainless steel, Ti-5Al-25Sn ELI, and OFHC copper. The program was divided into the following phases: (1) Variation of H Hydrogen-Environment Embrittlement with Material Condition for Inconel 718. Tensile tests on notched specimens were used to determine the effect of as-received material condition, heat treatment, and welding on the hydrogen-environment embrittlement of Inconel 718 in 5,000 psi hydrogen at room temperature; (II) Tensile Properties of Alloys in Hydrogen Environments, The effect of 5,000 psi hydrogen on the tensile properties of the alloys listed abovo was determined at room temperature and -200 F; (III) Threshold Stress Intensity of Alloys in Hydrogen Environments. Threshold stress intensities for the alloys listed above and in addition 2219-T87 aluminum alloy were determined with modified WOL specimens for a hydrogen pressure of 5,0υ psi and room temperature.

Unclassified
Security Classification

KEY WORDS	LINK A		LINK B		LINK C	
	ROLE	WT	ROLE	WT	ROLE	WT
nbrittlement						
otch Tensile Properties						
eld Metal/Parent Metal						
eat-Affected Zones						
racture Toughness						
ransverse Sections						
nconel 718						
nconel 625						
ISI 321 Stainless Steel						
i-5Al-2.5Sn ELI						
FHC Copper						

Unclassified
Security Classification